Development of alternative diagnostic protocols for *Candidatus* Phytoplasma asteris and *Coniella granati* Sacc. (Syn. *Pilidiella granati*)

by

Lucan Dylan Page

Thesis presented in partial fulfilment of the requirements for the degree of Master of Science in Genetics in the Faculty of Natural Sciences at Stellenbosch University

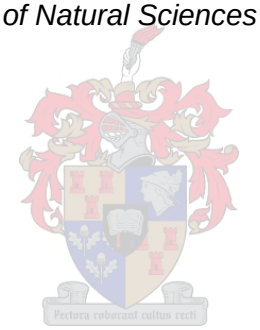

Supervisors: Prof. Johan T. Burger, Prof. Umezuruike Linus Opara
Co-supervisors: Prof. Willem J. Perold, Prof. Hans J. Maree

April 2019

Declaration

By submitting this thesis electronically, I declare that the entirety of the work contained therein is my own, original work, that I am the sole author thereof (save to the extent explicitly otherwise stated), that reproduction and publication thereof by Stellenbosch University will not infringe any third-party rights and that I have not previously in its entirety or in part submitted it for obtaining any qualification.

Date: April 2019

Abstract

The Republic of South Africa (RSA) is an integral part of the global fruit exporting chain. Currently, South Africa is ranked eighth in the world in wine production, exporting 40% of all locally produced wine. Another emerging fruit industry is pomegranates, of which RSA currently ranks fourth in the Southern hemisphere, exporting 88% of its pomegranate produce. However, pathogens affect the yield of these industries, warranting further research. Two of these pathogens are *Candidatus* Phytoplasma asteris (AY phytoplasma), a phytoplasma that infects grapevine, and *Coniella granati*, a fungus that infects pomegranates. AY phytoplasma was first reported in RSA in 2010 and *C*. *granati* was first reported in RSA in 2017. Currently, methods used for the detection of both pathogens rely on time-consuming nested-PCR assays that require trained technicians and equipment such as thermocyclers.

The aim of this project was to develop a functional diagnostic method for the rapid detection of AY phytoplasma and *C*. *granati*. This project also aimed to compare current diagnostic assays to a new isothermal diagnostic assay, namely recombinase polymerase amplification (RPA). Additionally, this project in collaboration with the department of Electronic and Electrical Engineering at Stellenbosch University is developing a microfluidic device for detection of these fruit pathogens, based on the RPA assay.

Isothermal RPA diagnostic assays for both AY phytoplasma and *C*. *granati* worked rapidly, effectively decreasing the time required to determine results. Comparisons between PCR and RPA diagnostic assays determined that PCRs were slightly more sensitive; however, the RPA was much faster. *In situ* tests of disease symptomology of pomegranate fruits replicated results found in literature. The biological groundwork for the microfluidic device was also laid; this was done by means of specificity tests, using biotinylated capture probes and streptavidin-coated magnetic beads.

This study advances the understanding of modern diagnostic assays compared to traditional diagnostic assays, reporting effective detection of plant pathogens in a short time. Overall, the RPA diagnostic was faster at detecting *C. granati* than the PCR, saving an estimated hour from start to finish, while the AY RPA successfully detected AY phytoplasma in an hour and twenty minutes compared with ten hours using the AY nested-PCR assay.

Opsomming

Die Republiek van Suid-Afrika (RSA) is 'n integrale deel van die globale vrugte uitvoerketting. Veertig persent van alle plaaslik geproduseerde wyne word uitgevoer. en Suid-Afrika is die agste grootste wynprodusent. 'n Opkomende vrugtebedryf in Suid-Afrika is granate. Suid-Afrika is tans die vierde grootste granaatprodusent in die suidelike halfrond en 88% van alle granaatprodukte word uitgevoer.

Patogene beïnvloed egter die opbrengs en oeste van hierdie industrië, daarom word verdere navorsing geregverdig. Twee van hierdie patogene is *Candidatus* Phytoplasma asteris (AY fitoplasma), 'n fitoplasma wat wingerde infekteer, en *Coniella granati*, 'n swam wat granate infekteer. AY fitoplasma is in 2010 en *C*. *granati* is in 2017 vir die eerste keer in SA gerapporteer.

Tans is diagnotiese metodes wat gebruik word vir die diagnosering van beide patogene, afhanklik van tydrowende polimerase ketting reaksies (PKRs), wat opgeleide tegnici en toerusting, soos termosikleerders, benodig om uitgevoer te word.

Die doel van hierdie projek was om 'n funksionele deteksie metode te ontwikkel vir die vinnige identifisering van AY fitoplasma en *C*. *granati*. Hierdie projek het ook daarop gefokus om huidige diagnostiese toetse te vergelyk met ‘n nuwe isotermiese diagnostiese toets, naamlik rekombinase polimerase amplifikasie (RPA). Daarbenewens ontwikkel hierdie projek in samewerking met die department van Ingenieurwese by die Universiteit Stellenbosch 'n mikrofluidiese toestel vir die indentifisering van hierdie vrugtepatogene.

Isotermiese RPA diagnostiese toetse vir beide AY fitoplasma en *C*. *granati* het vinnige resultate gelewer. Dus was effektief minder tyd van begin tot einde benodig vir suksesvolle identifikasie van bogenoemde patogene. Vergelykings tussen PKR diagnostiese toetse en RPA diagnostiese toetse het bepaal dat PKR’s effens meer sensitief was, maar die RPA was heelwat vinniger. *In situ* toetse van die simptome van siektes van granaatvrugte het die resultate in literatuur bevestig. Die biologiese fondasie vir die mikrofluidiese toestel is ook gelê met behulp van spesifisiteits-toetse gebiotinileerde DNS-fragmente en streptavidien-bedekte magnetiese sfere te gebruik.

Hierdie studie bevorder die kennis van moderne diagnostiese toetse relatief tot tradisionele diagnostiese toetse, en rapporteer effektiewe identifikasie van plantpatogene binne 'n kort tydsbestek.

Acknowledgments

I would like to extend my sincere appreciation towards the following people and institutions for their various contributions towards this study:

- My supervisor, Prof. J.T. Burger, for giving me an opportunity to explore my passion for science. I'd like to thank him for his patience and guidance and giving me my first glass of proper red wine.
- My co-supervisor, Prof. H.J. Maree, for his intellectual inputs and guidance along my multiple years in the lab.
- My co-supervisors, Prof. U.L. Opara and Prof. W.J. Perold for making this project a possibility.
- Members of the Vitis Laboratory, for the stimulating and uplifting working environment, keep that Disney spirit alive.
- Rebecca Tunstall, for her friendship, motivation, and being my rock. For wine adventures and always being there, in my times of need.
- Kristin Oosthuizen, for her friendship and constant assistance and encouragement throughout this study, for our walks and impromptu rants.
- Ané Kruger, for friendship, guidance, and helping me find my feet in the lab.
- Dr Clint Rhode and Dr Barbara van Asch for philosophical debates and steak lunches.
- My family and friends, for their moral and financial support.
- The department of Genetics at Stellenbosch University for giving me a platform to excel in.
- The Department of Trade and Industry (DTI), AgriEdge and Tropicsafe, for research funding.
- SARChI Postharvest Technology for the award of the National Research Foundation (NRF) grantholder-linked bursary.

Table of contents

Contents

List of figures

List of tables

List of Abbreviations

3’ – three prime

5’ – five prime

A - adenine

AY – Aster Yellows

BLAST – Basic Local Alignment Search Tool

Bp – base pair(s)

C - cytosine

Ca. – *Candidatus*

CAF – Central analytical facility

CG – control group

CTAB – cetyltrimethylammonium bromide

DNA – deoxyribonucleic acid

DOI – digital object identifier

EDTA – ethylenediaminetetraacetic acid

ELISA – enzyme linked immunosorbent assay

EPPO - European and Mediterranean plant protection organization

EU – European Union

F – forward primer

G – guanine

GDP – gross domestic product

IG – internally inoculated group

IMP – immunodominant membrane proteins

IPTG – isopropyl β-D-1-thiogalactopyranoside

ITS – internal transcribed spacer

kb – kilobase(s)

LB – Luria-Bertani

LFD- lateral flow dipstick

LFD-RPA – lateral flow dipstick recombinase polymerase amplification

MgOAc – magnesium acetate

MLO – mycoplasma-like organism

MRSA - methicillin-resistant *Staphylococcus aureus*

NCBI – National Center for Biotechnology Information

NTC – no template control

PCR – polymerase chain reaction

PDA – potato dextrose agar

PVP-10 – polyvinylpyrrolidone-10

qPCR – quantitative PCR

R – reverse primer

rDNA – ribosomal deoxyribonucleic acid

RFLP - restriction fragment length polymorphism

RNA – ribonucleic acid

RNase – ribonuclease

RO – reverse osmosis

RPA- recombinase polymerase amplification

RSA – Republic of South Africa

Sacc – Saccardo

SAWIS – South African Wine Industry Information and Systems

SG – surface inoculated group

T- thiamine

Taq – *Thermus aquaticus*

tuf – elongation factor Tu

v/v – volume per volume

w/v – weight per volume

WHO – World Health Organization

X-gal – 5-bromo-4-chloro-3-indolyl-β-D-Galactopyranoside

Chapter 1 – Introduction

1.1 General introduction

The fruit industry is a major contributor to the South African economy. Two important crops are grapevine (*Vitis vinifera*) and pomegranates (*Punica granatum*). As of 2017 the grapevine industry of RSA comprised of an estimated 119,181 hectares of vineyards, of which 94,545 hectares are dedicated to wine production. SA ranks eighth in the world in wine production, producing 1.08 billion litres of wine, of which 448.4 million or 41.5% was exported[1]. The South African wine industry contributed 1.2% of the GDP and employed 290,000 people in 2013[2]. In 2017 the pomegranate industry of RSA had an estimated 826 hectares planted to pomegranates, producing 5,813.44 tons of pomegranate produce, with 5,115.83 tons, or 88%, being exported[3]. Currently the South African pomegranate industry is ranked 4th out of the Southern hemisphere producers, trailing behind producers in the Northern hemisphere[3,4].

Plant pathogens affect the yield of both grapevines and pomegranates. These include *Candidatus* phytoplasma asteris and *Coniella granati*, synonym *Pillidiella granati*. *Candidatus* phytoplasma asteris, colloquially known as aster yellows is a pathogenic cell wall-less mollicute infecting grapevine. Symptoms of aster yellows infection include yellowing of the leaves, shortened internodes and incomplete lignification[5,6], all contributing to severe yield loss. *Coniella granati* is a pathogenic fungus that causes postharvest heart rot in pomegranates, making the fruits unusable[7,8].

Currently, detection methods for both pathogens require trained technicians to detect and diagnose infections. These detection assays range from nested-polymerase chain reactions (PCRs)[6,9] to enzyme-linked immunosorbent assays (ELISAs)[10]. These assays are time consuming and require an equipped laboratory. Recently, isothermal techniques, such as recombinase polymerase amplification (RPA) and loop-mediated isothermal amplification (LAMP), have been used to detect pathogens ranging from viruses[11] to fungi[12]. These detection assays have been shown to be effective, both faster[13] and more sensitive[14] than traditional methods, and simple enough for a layperson to use. Further studies have indicated that RPA diagnostic assays could also be translated to lab-free, on-site, point-of-care use by means of

microfluidic/electronic devices, ranging from lateral flow dipsticks to fully automated electronic devices[14,15].

1.2 Project proposal

The aim of this project was to develop a functional diagnostic method for the rapid detection of *Candidatus* Phytoplasma asteris and *Coniella granati* (Syn. *Pilidiella granati*). This project aimed to compare RPA diagnostic assays to PCR diagnostic assays. Furthermore, this project also aimed to lay the groundwork for a microfluidic/electronic device for the detection of these pathogens.

The aims were investigated by means of the following objectives:

- Create a plasmid control construct using *Candidatus* Phytoplasma asteris DNA.
- Compare PCR vs RPA using the control construct.
- Design an RPA diagnostic for *Candidatus* Phytoplasma asteris.
- Design an RPA diagnostic for *Coniella granati* Sacc (Syn. *Pilidiella granati*)
- Test RPA diagnostic in detecting both *Candidatus* Phytoplasma asteris and *Coniella granati* in different backgrounds i.e. water and juice/plant sap.
- Lay groundwork for extrapolating the diagnostic assays to an electronic/microfluidic device.

This study, in collaboration with the Department of Electronic and Electrical Engineering and SARChI Postharvest Technology section in the department of Horticulture at Stellenbosch University, will aim to develop a microfluidic device for the detection of two plant pathogens, *Candidatus* Phytoplasma asteris and *Coniella granati*.

1.3 Chapter layout

Chapter 1: General introduction, the project proposal including the aim and objectives, as well as the chapter layout.

Chapter 2: Literature review relating to grapevine and pomegranate statistics, current diagnostic methods for both *Candidatus* Phytoplasma asteris and *Coniella granati*, and current implementations of microfluidic devices.

Chapter 3: Materials and Methods.

Chapter 4: Results and Discussion.

Chapter 5: General conclusion.

Chapter 2 – Literature Review

2.1 Global fruit importance

Fruit is one of the most valuable food commodities globally, making up a large part of human and animal diets. Fruit contains large quantities of fibre, vitamins, and antioxidants required for healthy living, and a lack of these essential dietary requirements leads to poor health conditions, under-development in children, and in severe cases, even death[16,17]. According to the World Health Organization (WHO), a dietary deficiency in fruits and vegetables leads to increases in noncommunicable diseases, such as cardiovascular disease, coronary heart disease and cancer[16–18]. In 2013, more than five million deaths were attributed to the lack of dietary fruits and vegetables[16]. It is estimated that a healthy diet should consist of at least 400 g of fruit and vegetable intake of which at least 160 g consists of fruit, daily[16–18]. Two fruit crops that are of global importance and are the focus of this study are grapevine, *Vitis vinifera* L., and, a growing, pomegranate, *Punica granatum* L, market.

2.2 Importance of grapevines and pomegranates in South Africa

2.2.1 Grapevine (*Vitis vinifera* L.)

Grapevine (*Vitis vinifera* L). is one of the RSA's most important crop species and is used for a wide range of products such as wine, table grapes, raisins and oil, and is also being studied for its use in the pharmacological industry, due to its potent antioxidants, anti-inflammatory, anti-aging and cardioprotective effects[19–21]. As of 2017, South Africa had an estimated 123,397 hectares of vineyards, of which 98,594 hectares were dedicated to wine grapes[1]. South Africa ranks eighth in the world in wine production, producing 918.6 million litres in 2017, of which 448.4 million or 48.8% was exported[1]. In 2013 the South African wine industry contributed 1.2% of the country's gross domestic product (GDP) and employed 289,151 people[2]. One of the biggest threats the grapevine, and more specifically the wine industry, has been pathogens. These pathogens include viruses, phytoplasmas, bacteria and fungi. One of these phytoplasma pathogens is *Candidatus* Phytoplasma asteris, also known as Aster Yellows (AY) phytoplasma.

2.2.2 Pomegranates (*Punica granatum* L.)

Pomegranate (*Punica granatum* L.) is an economically important crop species around the world was well as being a fast growing market in RSA[3]. Pomegranates were first cultivated in what is now known as Iran, and were subsequently spread globally due to its many sought after qualities[22]. The arils of the fruit, which are the sweet and juicy part around the seeds, are of greatest value. They are utilised for various purposes such as food, pharmaceutical, and cosmetic products[22,23]. In 2012, RSA had an estimated 780 hectares of pomegranate crops; this grew to an estimated 826 hectares by the end of 2017, a growth rate of 5%, with a further 22% growth in production area estimated by 2022[3]. It is estimated that by 2023 pomegranate popularity will rise from the18th most consumed fruit annually, to the 10th most consumed, subsequently increasing its economic importance[3]. In RSA, the harvest times of pomegranates range between February and June[24]. Pomegranates are threatened by many pathogens that affect both the fruit and other plant organs at various stages of production. These pathogens range from viruses, to bacteria and fungi, one of which is *Coniella granati* (syn. *Pilidiella granati*).

2.3 Local influence of pathogens

2.3.1 Phytoplasma: *Candidatus* Phytoplasma asteris

2.3.1.1 Background

Candidatus (*Ca.*) Phytoplasma asteris are phloem-limited mycoplasma-like organisms (MLO), considered to be part of a group of prokaryotic pathogens associated with Aster Yellows (AY) disease[6,25]. AY disease affects many different herbaceous dicotyledonous and monocotyledonous plants[26]. Phytoplasma spp. were first reported in China causing “Yao yellow-kind” phenotype in peonies, a thousand years ago, where the disease was actively promoted for aesthetic reasons[27]. However, when the disease is present in crop plants it is associated with disruptions in nutrient flow in phloem cells[28], which leads to yield loss in many cases and, when left unattended, to death.

Grapevine is one of the most economically important crop species globally. It is affected by phytoplasma spp., which lead to Grapevine Yellows (GY) disease[5,6,26]. Although phytoplasma spp. have been reported in many parts of the world, this does not necessarily include those species that infect grapevines. Countries that have

reported phytoplasma spp. in grapevine include Australia[29,30], Chile[31,32], Croatia[33], France[34], Germany[35], Greece[36], Hungary[37], Iran[38], Israel[36], Italy[36,39], Portugal[40], Slovenia[41], South Africa[42,43], Spain[44,45], Switzerland[45,46] and Turkey[47], as visualised in Figure 2.1.

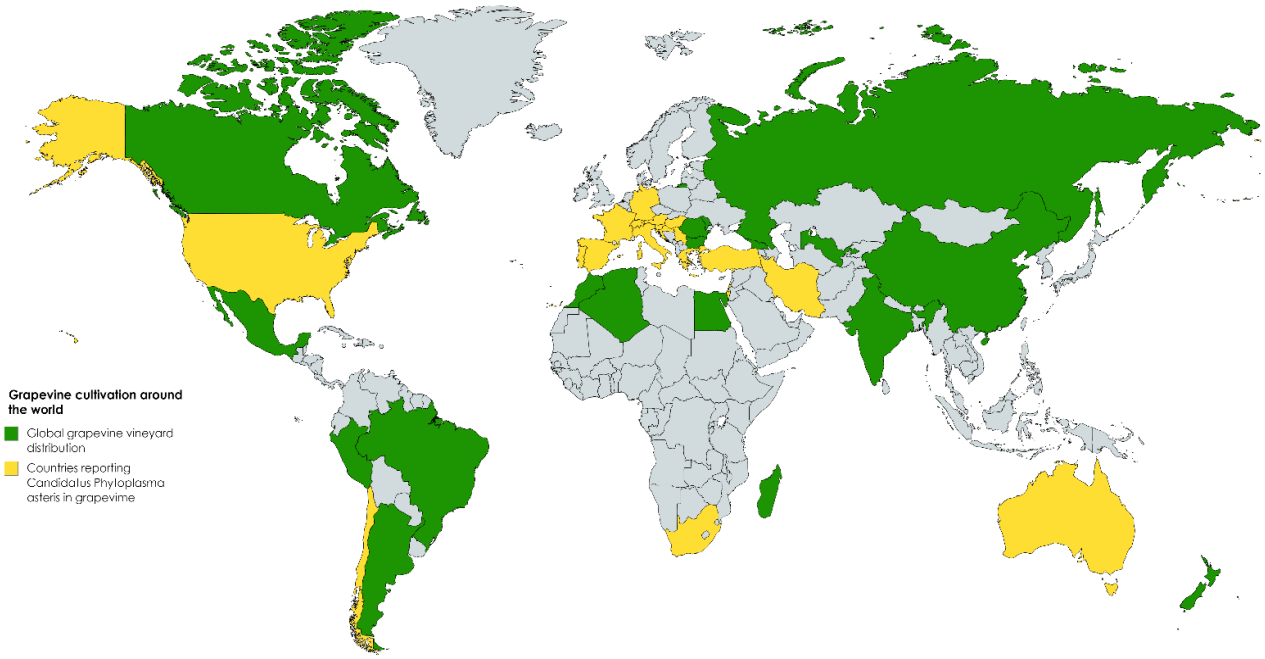

Figure 2.1 - Global distribution of grapevine cultivation. Yellow indicating countries that have reported *Candidatus* Phytoplasma asteris infecting grapevines. Green indicating countries unaffected by *Candidatus* Phytoplasma asteris.

2.3.1.2 Economic impact of AY infection

The economic impact of phytoplasma spp. can be great, in the 1950s a phytoplasma outbreak in France, coupled with a lack of pest control, lead to the number of infected plants exponentially increasing and spreading towards neighbouring countries. This led to it being classified in the European Union (EU) as a harmful organism and subsequently listed as an A2 quarantine organism by the European and Mediterranean Plant Protection Organization (EPPO)[48]. Currently, no estimates of the total economic loss attributed to phytoplasma spp. exist; however, due to disease symptoms, such as abortion of the fruit bunches, if the disease is left unchecked, it could be deduced that innumerable losses could probably ensue.

2.3.1.3 AY Characteristics

2.3.1.3.1 Morphological characteristics of AY phytoplasma

Candidatus Phytoplasma asteris are pleiomorphic, cell wall-less pathogenic prokaryotes ranging between 100 and 800nm in diameter[6,49,50]. Figure 2.2 depicts the morphological structure of phytoplasmas in phloem cells as imaged by a transmission electron microscope[6,51].

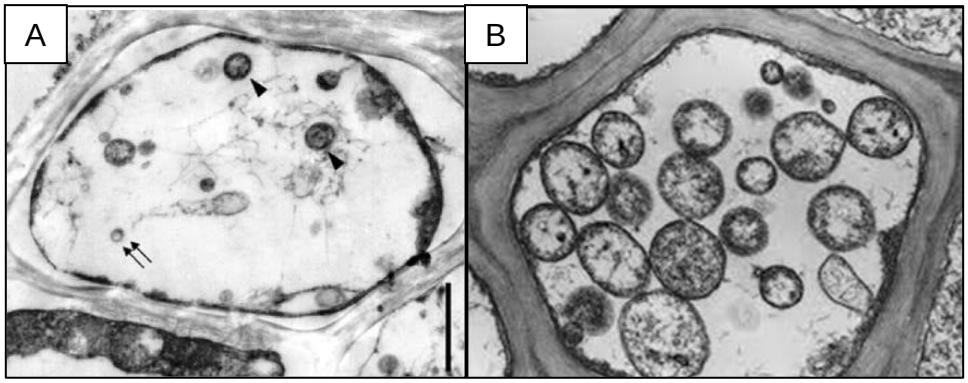

Figure 2.2 – A - depicts pleiomorphic Phytoplasma structures in a bamboo leaf phloem-cell as electron micrograph taken by Jung *et al.*[51] indicated by arrows; B - depicts a plant phloem-cell infected by Phytoplasmas[25].

2.3.1.3.2 Taxonomy of Aster Yellows phytoplasma

Currently, phytoplasmas cannot be routinely cultured *in vitro*, subsequently Koch's postulates cannot successfully be applied, therefore they are provisionally categorised under *Candidatus* phytoplasma species[52,53]. Therefore, different species of phytoplasma must be characterised by means of genetic sequence analyses. Phytoplasma spp. have genome sizes ranging from 530 to 1,200 kilobases (kb), with a GC content ranging from 23 to 29% and consisting of an estimated 839 protein coding genes of which 337 genes remain unassigned[53]. Possible mobile units (PMUs) have also been discovered in phytoplasmas; these plasmids may enhance genetic plasticity[52]. Accumulation of PMUs can lead to genomic modification and subsequent change in phenotypic expression[52]. Historically, phytoplasmas with known 16S rDNA sequences were characterised into 20 distinct phylogenetic clades. Restriction fragment length polymorphism (RFLP) analyses led to the classification of 75 distinct phytopathogenic mollicutes[54].

Currently, an identification scheme exists that is based on RFLP analyses of the 16S rDNA gene sequence, as well as the Tu elongation factor (*tuf*), *ribosomal protein* (*rp*),

bacterial chaperone *groEL*, *antigenic membrane protein* (*amp*), and protein translocase subunit *SecY* gene sequences[52,53,55–57]. RFLP analyses of phytoplasma spp. led to the identification of 32 16S ribosomal (16Sr) groups, which collectively consist of more than 200 subgroups[52], regarded as one the most genetically diverse species, occupying many different niches, according to Lee *et al*.[56]. AY phytoplasmas are classified in group 16Srl, which comprises 15 subgroups, with most pathogenic AY phytoplasmas falling in subgroups 16Srl-A and 16Srl-B[52,56].

2.3.1.4 AY phytoplasma Infection cycle

AY is spread between different plant hosts by means of insect vectors. These insects comprise mostly of leafhoppers, found in the order: Hemiptera[43,58,59]. In the RSA the primary AY insect vector in grapevine was identified as *Mgenia fuscovaria* (Figure 2.3)[43,60]. Leafhoppers feed on plant sap, found in vascular tissues of different plant species. These insects become exposed to phytoplasma when feeding on infected plants. Insects have to feed on infected plant material for minimum time period, known as the acquisition access period (AAP), for them to become infectious[61]. Once phytoplasmas have been acquired by the insect vector, a latent period is entered, during which the phytoplasma replicates in the salivary glands[61]. Hereafter, by probing uninfected plants, these leafhoppers are able to transmit the phytoplasma, also completing the life cycle[61,62,63]. The transfer of phytoplasmas is most effective by leafhoppers while in their early developmental stages[64]. A study done by Beanland *et al*.,2000. indicated that leafhoppers that were carriers of phytoplasma spp. had a greater evolutionary fitness when compared to those that were not carriers, living between 36 and 47% longer. Leafhoppers that were carriers also had twice the number of offspring, when compared to their counterparts, the uninfected leafhoppers[64].

Figure 2.3 – Leaf hopper *Mgenia fuscovaria*, the main vector for the spread of *Candidatus* Phytoplasma asteris in grapevine, in South African vineyards, courtesy of K. Kruger, University of Pretoria

2.3.1.5 Symptomology of AY infection

Because *Ca.* Phytoplasma asteris disrupts nutrient flow in plants, it may be difficult to distinguish the resultant symptoms from those of abiotic environmental factors. However, characteristic symptoms, associated with AY infection, have been identified in grapevines - these include yellowing and curling of the leaves, shortened internodes, incomplete lignification, and abortion of young leaves and fruit bunches[5,42,65]. These symptoms can be seen in Figure 2.4.

Figure 2.4 –A - depicts yellowing of the leaves as well as curling of the edges as taken by the Saguez[65]; B - depicts shortened internodes, incomplete lignification of the canes, and curling and yellowing of the leaves, image courtesy of J. Burger; C - depicts an aborted grape bunch. Adapted from Carstens[60].

2.3.1.6 Current diagnostic methods for detection of AY

Currently, several diagnostic techniques exist for the detection of phytoplasma spp.; these include transmission electron microscopy (TEM)[25], ELISA[10,66], PCR[67,68], and qPCR [67–69]. All these diagnostic techniques have advantages and disadvantages. For example, TEM requires a trained professional, it is time consuming, and cannot differentiate between subgroups, simply relying on morphology[70]. ELISA is simple and can process multiple samples at the same time, making use of antibodies to detect specific *secA* membrane proteins, as well as other immunodominant membrane proteins (IMPs); however, not all strains of phytoplasma have these specific membrane proteins, potentially leading to false negatives[70]. PCR assays have been the diagnostic of choice among researchers and pathologists, specifically nested-PCR assays that are able to detect extremely low titre pathogens, such as AY in grapevine. This approach makes use of three separate PCR amplifications, each amplifying the product of the previous PCR i.e. amplicon two is amplified from amplicon one, and amplicon three amplified from amplicon two[6]. The nested-PCR approach is time consuming and prone to contamination. It was found by Smyth[71] that the nested-PCR approach was more effective than qPCR as a diagnostic assay, being able to detect pathogens a thousand times less concentrated than the Taqman qPCR approach.

2.3.2 Fungi: *Coniella granati*

2.3.2.1 Background

Coniella granati, formerly known as *Pilidiella granati*, has been reported in China[72], Greece[73], Italy[74], Iran[75], Mexico[7], South Africa[76], Spain[77], and the USA[8,78] as an aggressive fungal pathogen that affects not only plant organs, such as the leaves and stems[76,79], but also the fruit, pre- and postharvest. Figure 2.5 indicates the global distribution of pomegranates reportedly infected with *C. granati*. There is currently no information regarding the original discovery of the pathogen, however the first reported incidence was in Spain in 2010[77].

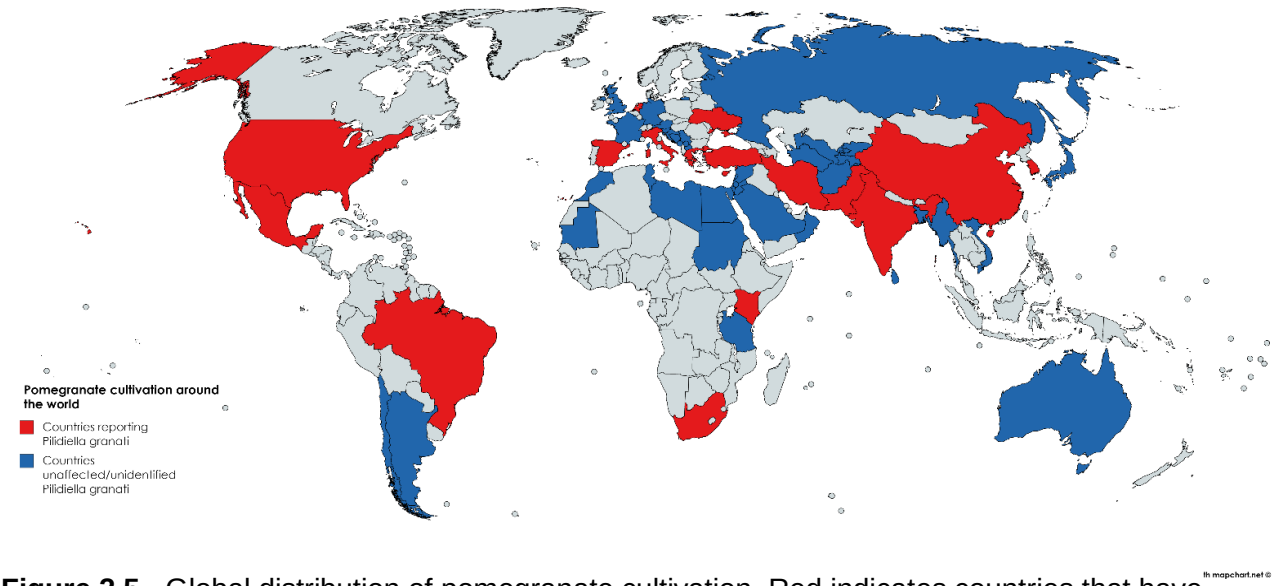

Figure 2.5 - Global distribution of pomegranate cultivation. Red indicates countries that have reported *Coniella granati* infecting pomegranates. Blue indicating countries unaffected by *Coniella granati* at the time of this study.

2.3.2.2 Economic impact of *Coniella granati* infection

The total economic impact of *C. granati* is still under investigation however, infections have been reported at incidence levels between 10 and 60% in different pomegranate orchids across the globe[73,77,80,81]. In 2016, 26% of fruit harvested were reported to have been infected with *C. granati* in Italy[74]. Infected trees tend to die after infection, and infected fruits are rendered useless, clearly demonstrating that *C. granati* has a major economic impact on the pomegranate industry.

2.3.2.3 Characteristics

2.3.2.3.1 Morphological characteristics of *Coniella granati* in culture

In culture *C. granati* produce white to cream-coloured colonies of velvety appearance with black concentric rings of pycnidia. Pycnidia are solitary and globulose, with thin, membranous, pseudoparenchymic walls up to 140 µm in diameter. Hyphae are septate, while conidia are hyaline, one-celled, ellipsoid to fusiform and on average 11.4-17.5 by 4.4-6 µm in size[73,77,81], this can be seen in Figure 2.6.

Figure 2.6 - *Coniella granati* grown on potato dextrose agar depicting clear black concentric rings of pycnidia; photo taken for the purposes of this study.

2.3.2.3.2 Taxonomic characteristics of *Coniella granati*

Currently no complete genome sequence of *C. granati* exists, however the focus of all current diagnostic assays has been on the internal transcribed spacer (*ITS*) 1, for which partial gene sequences exist, as well as the 5.8S ribosomal RNA gene and *ITS2*, for which complete sequences exist. Further, a partial sequence for the 28S ribosomal RNA gene exists. The *ITS1* and *ITS2* regions are however used when barcoding individual species and is thus an ideal DNA region to base a diagnostic assay on, as it is both conserved enough to detect a specific species, but diverse enough to differentiate between strains.

2.3.2.4 Coniella granati infection cycle

Two methods of infection have been hypothesised, these include infection of young trees and fruit, causing necrosis and crown rot, or envelopment of fungal spores in fruit, causing heart rot. The first process of infection is initiated when single-celled pycnidiospores are disseminated by wind and water. Once these spores encounter young pomegranate trees and fruit, a fungal colony is formed. If contact is made with fruit, necrosis of the fruit occurs that starts as the sepals develop; this is known as crown rot. If fungal colonies form on young trees, necrosis starts on the lower part of the stem, causing dieback of young branches and roots[82]. Once fungal colonies have matured, *C. granati* starts developing new spores. These spores overwinter in dead branches and mummified fruits until the start of the next season, when the cycle

continues[82]. Another hypothetical method of infection is that spores travel with pollen during the flowering stage of pomegranate trees[83]. This leads to the spores being enveloped by the fruiting bodies. Once inside the fruit, *C. granati* propagates and causes a disease known as heart rot. When affected with heart rot, the fruit look normal in appearance from the outside, but are rotten on the inside[83,84].

2.3.2.5 Symptomology of *Coniella granati* infection

Symptoms of *C. granati* infection varies depending on the site of infection. Pomegranate trees that have been infected at the lower part of the stem, typically show signs of twig dieback, necrosis of the tree, and eventual death of both young branches and young trees (7 to 10 years)[73,77,80,81,85], as can be seen in Figure 2.7 (D). Pomegranate fruits that have been infected show distinct signs of crown rot, both pre- and postharvest. Figure 2.7 (A to C) are indicative of Crown rot[77,86].

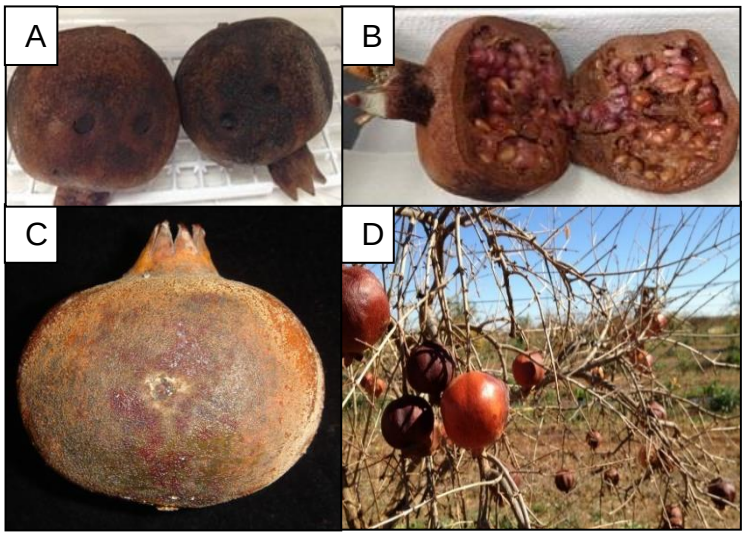

Figure 2.7 – Images of crown rot in pomegranate fruit – A to C are *C. granati* artificially infected pomegranate fruits. Pomegranate stem dieback is depicted in image D by Smith[85].

2.3.2.6 Current diagnostic methods for the detection of *Coniella granati*

Currently, there are three ways of detecting *C. granati*: First, morphological identification is used to identify *C. granati* on a potato dextrose agar (PDA) plate by means of comparison to known samples, as described in section 2.3.2.3.[7,76]. The second are nested-PCR assays, which focus on amplifying the ITS1, ITS2, and the 5.8S rDNA regions of the *C. granati* genome[76,82]. The nested-PCR assay consists of two primer sets. For the first round of PCRs, a universal primer set, ITS1 and ITS4,

amplifying partial 18S rDNA and partial 28S rDNA regions respectively, is used. The product of this PCR is used in the second round of amplification, where the second primer set, namely S1 and S2 is used to amplify a 450 bp product. Figure 2.8 indicates the overlap and positioning of the two primer sets[82].

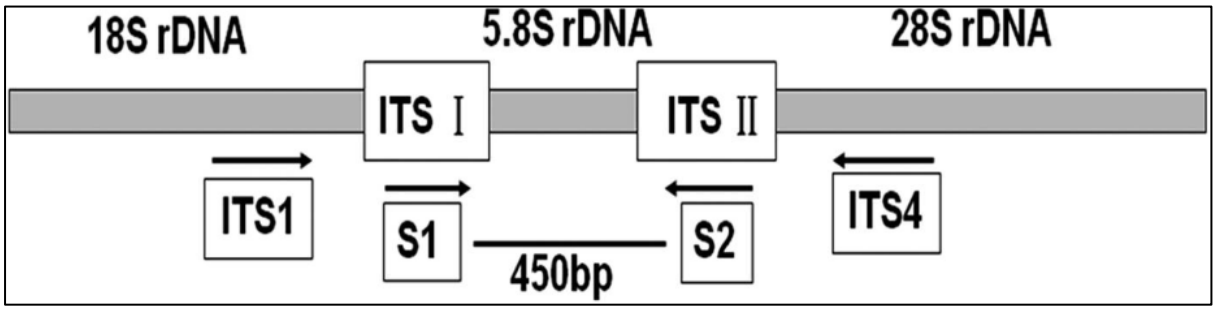

Figure 2.8 – Diagram of the nested-PCR approach, as described by Yang *et al*.[82]

And finally, pathogenicity tests are used for detection of *C. granati*, these follow Koch's postulates, where a pomegranate tree or fruit is manually infected using fungal plugs and observed for identifiable symptoms of *C. granati* infection, as described in section 2.3.2.5.[7,76,81].

2.4 Recombinase Polymerase Amplification (RPA)

2.4.1 Background

Recombinase polymerase amplification (RPA) is the pioneering product of the American company, TwistDx™, which was first established in 1999[87]. RPA was developed as an isothermal amplification method that is both highly selective and sensitive[88]. It provides an alternative approach to the thermocycling of a traditional polymerase chain reaction (PCR), operating optimally at a single temperature ranging from 37°C to 42°C, but, also shown to work at room temperature[13,88,89]. The isothermal qualities of an RPA provide an ideal detection method for underequipped environments, such as on-site diagnostics or point-of-care devices[13,15,89–91]. In 2006, Piepenburg *et al*. published a study where they expanded the capabilities of the RPA diagnostic assay when detecting methicillin-resistant *Staphylococcus aureus* (MRSA). The authors of this study set out to establish a point-of-care system that was equally, if not more efficient, than the diagnostic assays available at the time. The authors developed an RPA system that was linked to fluorophores, where positive results could be detected using a handheld fluorometer. An even simpler detection method was also developed in the same study using RPA lateral flow dipsticks, which would

indicate a positive result by means of a visible line, making use of biotin-labelled RPA oligonucleotides and biotin specific antibodies[92] .

2.4.2 Mechanism of recombinase polymerase amplification

RPA functions by means of three important components; 1. A recombinase, specifically *Escherichia coli* recA; 2. DNA polymerase; and 3. single-stranded binding proteins (SSBs)[88,89,92,93]. The amplification starts when the bacterial recombinases pair a predesigned oligonucleotide primer with a homologous sequence on the DNA of the organism being targeted, as seen in Figure 2.9 (A). In Figure 2.9 (B) SSBs bind to the antisense DNA strand, stabilising the occurring D-loop. Subsequently, a strand displacing polymerase attaches to the primer-DNA complex and amplification starts as depicted in Figure 2.9 (C). This happens exponentially and if paired with a second primer on the opposing strand, an amplicon is formed, as seen in Figure 2.9 (D-E)[92]. This amplicon can then be assessed by using gel electrophoresis. Reverse transcriptase (RT) can be added to the RPA reaction mix; once added it is possible to amplify both DNA and RNA[94].

However, these enzymes, depending on the kit, are already provided in a single freeze-dried solution, patented by TwistDx™. Each 0.5 ml Eppendorf tube contains enough freeze-dried solution for a single reaction, to which rehydration buffer, PCR-grade water, the specific forward and reverse primers, the template DNA being tested, and finally magnesium acetate (MgOAc) that initiates recombinase binding[88], are added.

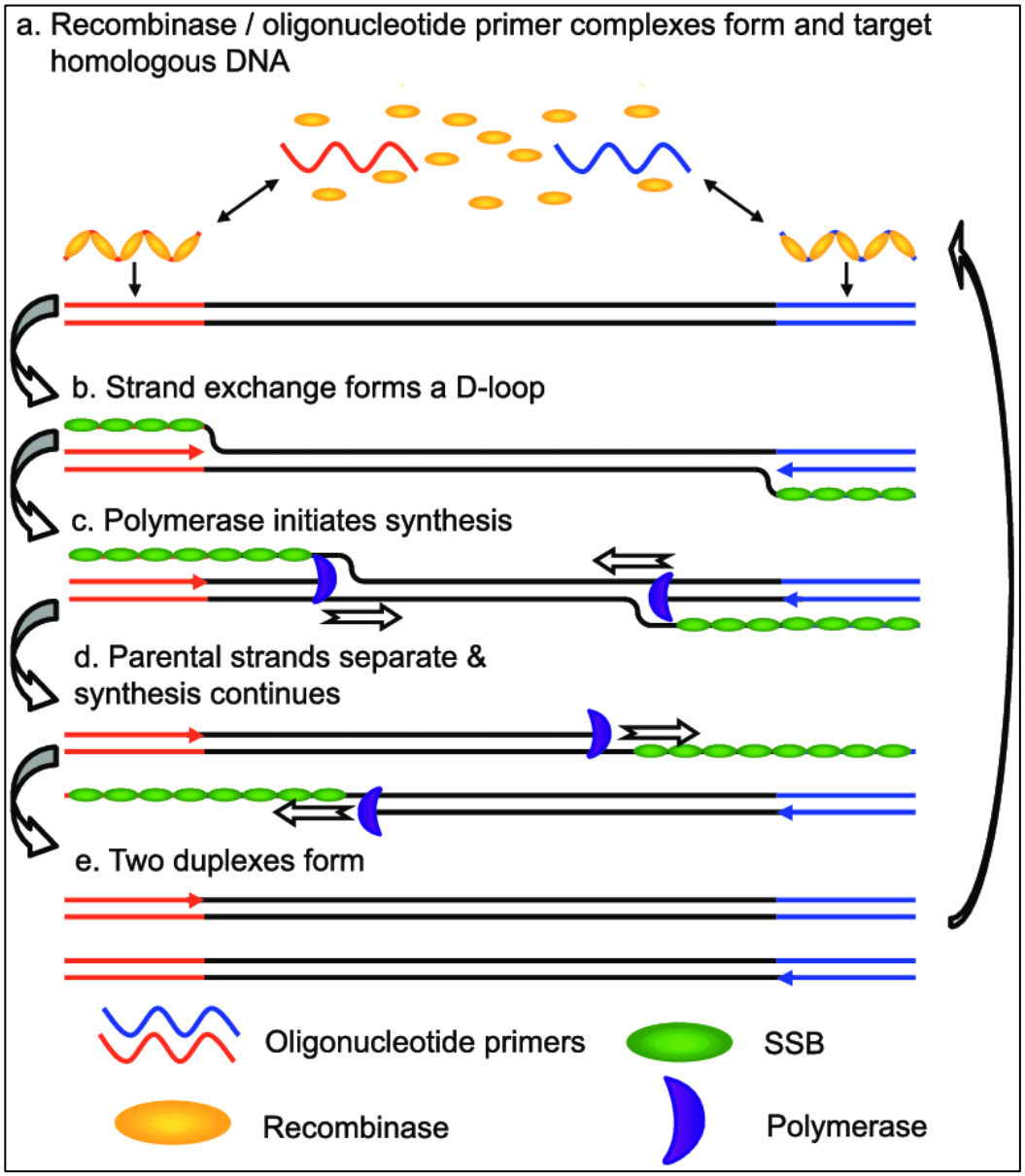

Figure 2.9 – Recombinase polymerase amplification (RPA) mechanism of amplification[13].

2.4.3 Current applications of RPA

Currently, multiple applications of RPA diagnostic assays are implemented, from virus detection using an RT-RPA method, to semi-quantitative analyses using fluorescently labelled RPA probes, to diagnostic DNA amplification. However, the biggest application for RPA has been in the field of pathogen detection. Recent studies employed RPA diagnostic assays for human related pathogens, such as human immunodeficiency virus (HIV)[95], foot-and-mouth disease virus (FMDV)[91], *Plasmodium falciparum* that causes Malaria[13], as well as biothreat panels (such as those testing for

Francisella tularensis, *Yersinia pestis*, *Bacillus anthracis*, Rift Valley fever virus, Ebola virus, Sudan virus, and Marburg virus)[90]. Recombinase polymerase amplification provides the solution for a fast, (typically around 20 minutes)[15,88,90,91], diagnostic test that can be implemented in rural areas, that lack expensive equipment, such as thermocyclers, and do not require trained diagnosticians/pathologists to operate.

Due to RPA's fast, sensitive, and accurate application in the detection of human pathogens, it became a viable diagnostic assay that could be utilised by plant pathologists; who often must resort to time consuming methods such as PCR or economical, but less sensitive enzyme linked immunosorbent assays (ELISA) to detect pathogens in plants. Quantitative real-time PCRs (qPCRs) are also frequently employed; however, this requires a skilled professional. RPA provides a viable alternative to these methods; being able to work at a single temperature makes it possible for laboratory-free diagnostic assays. Furthermore, it is highly sensitive, detecting as low as ten copies of DNA in solution[96], making it a promising avenue for diagnostics of low titre pathogens. A few studies have been performed to detect plant pathogens using RPA. RPA studies on plant viruses make use of crudely extracted nucleic acids which is favourable when considering on-location diagnostic testing. An example is a study done by Silva *et al*., 2018, showing the effectiveness of RT-RPA in detecting potyviruses from crudely extracted yam RNA[97]. Another study by Londoño, Harmon, and Polston, 2016, demonstrated the effectiveness of RPA for the detection of begomoviruses in a variety of plant hosts, finding it to be cheaper, faster, and more sensitive than an ELISA, but not as sensitive as a PCR, though still competitive[11]. These studies are further supported by Rojas *et al*., 2017, who developed an RPA diagnostic for the detection of *Phytophthora sojae* and *Phytophthora sansomeama*, which are pathogenic fungi causing root rot in soybeans. The authors found that although a qPCR was considerably more sensitive than an RPA, detecting 100 femtograms (fg) compared to the 10 nanograms (ng) limit of an RPA, the RPA was still more practical and consistently and reliably diagnosed infected plants[98].

2.4.4 Limitations of RPA

Recombinase polymerase amplification still has a few limitations that need to be mentioned. According to the TwistDx™ user manual, RPA has a limitation when it comes to detecting *E. coli* strains K12 and BL21, since these strains are used for

recombinant protein production, used in the kit[93]. Further limitations include RPA's high risk of contamination, being attributed to its isothermal nature and high sensitivity. This can be overcome by aseptic lab techniques. A final disadvantage is that a standard RPA still requires visualisation by gel electrophoresis, to determine results. This limitation can be overcome by combining an RPA diagnostic with a microfluidic device or using fluorochromes that become visible once amplification occurs.

2.5 RPA in association with microfluidic devices

Currently, RPA diagnostic results are assessed using gel electrophoresis, making RPA impractical for lab-free work. However, this has been addressed using several different microfluidic devices, ranging from simple lateral flow dipsticks (LFD)[99] to microfluidic electronic devices. Lateral flow dipsticks make use of biotinylated RPA primers and a paper strip coated with two label lines, as can be seen in Figure 2.10[14,92,100]. These label lines consist of two separate antibodies. One consists of a biotin-specific antibody and the other of a fluorophore-specific antibody. Target amplicons being screened for will contain both a fluorescein amidite (FAM) label as well as a biotin-label. Once the reaction mix is introduced into the sample pad α-FAM-gold dye molecules bind to the FAM labels. Subsequently, the reaction mix will move through the LFD membrane by means of osmosis, where it will interact with the two specific antibodies. Unbound α-FAM-gold dye molecules will interact with the control line, due to FAM-specific antibodies, indicating a functional LFD-experiment. FAM-Biotinylated DNA conjugates will interact with the biotin-specific antibody at the detection line, indicating a positive or negative result[14,100]. Only pathogen-specific amplicons will be detected as a result of biotin labels introduced during the isothermal amplification.

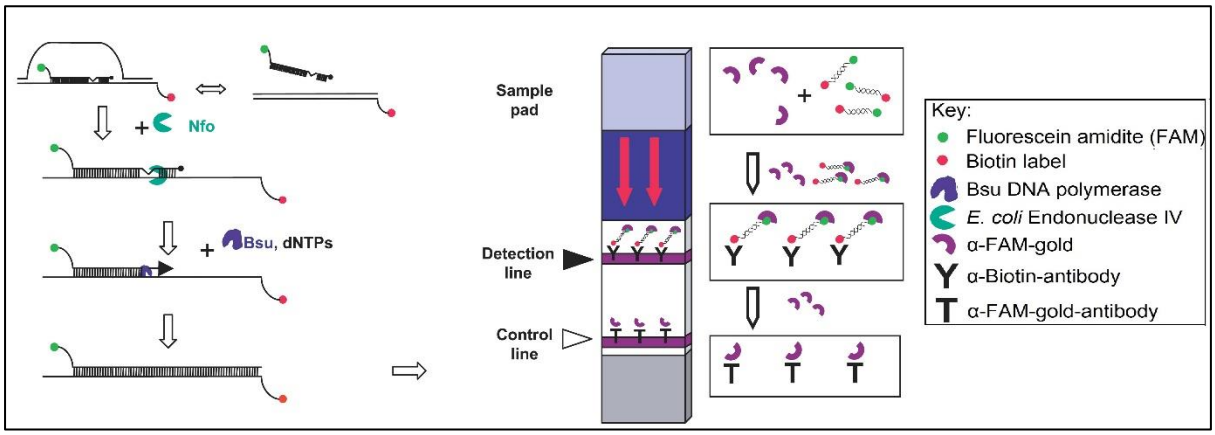

Figure 2.10 – Diagram of a lateral flow dipstick depicting RPA amplification, a sample pad, detection line, and a control line[92]

A few studies have used LFD-RPAs as a diagnostic alternative when doing on-site testing in resource-poor areas. A study by Sun *et al*.[99] showed the efficiency of LFD-RPAs in detecting *Schistosoma japonicum*, a blood parasite that causes schistosomiasis in mammals, including humans[99,101]. The authors showed that LFD-RPAs were sensitive, rapid and specific and could be visualised with the naked eye, which is beneficial for use at rural clinics[99]. Another study by Tu *et al*.[102] presented an LFD-RPA diagnostic to detect caprine arthritis-encephalitis virus (CAEV), a pathogenic lentivirus that causes arthritis in older goats and encephalitis in younger goats. They showed that LFD-RPA was more sensitive at detecting CAEV than a traditional PCR and ELISA, but also that the results were available in 35 minutes[102]. Both studies emphasised the potential of LFD-RPA for lab-free, on-site diagnostics[99,102].

More advanced microfluidic devices have also been developed to work in conjunction with RPA. These devices tend to focus on quantitative measurements, as opposed to qualitative or semi-quantitative measurements done by LFD-RPAs[99,102,103]. A study by Yeh *et al*.[103] described the development of a device known as self-powered integrated microfluidic point-of-care low-cost enabling (SIMPLE) chip, to quantitatively detect MRSA in human blood samples by means of digitally analysed fluorescence. The SIMPLE chip makes use of RPA to amplify MRSA DNA from a sample, and quantitatively assesses the severity of the infection. This device makes use of prepared RPA amplification mixes separated from MgOAc to prevent amplification and the occurrence of false positive results. Further features of the device include blood sample compartmentalisation and automated plasma separation, as well as vacuum

waste disposal of samples into a waste reservoir. Once a sample is loaded into the device, plasma is separated from the blood platelets. Plasma is then introduced into the RPA reaction mix, along with the MgOAc. The device then measures the level of fluorescence that occurs and digitally assesses the severity of the infection. Once the reaction is completed, the reaction mix is vacuum-disposed. This study showed that quantitative on-site devices, making use of isothermal RPA technology is possible and lays the foundation for future devices[103].

Another MRSA study by Lutz *et al.*[15], created a lab-on-a-foil system, implementing a custom blow-moulded cartridge that was sealed using adhesive tape. This cartridge contained RPA reagents, and by means of a centrifugal analyser (a device that makes use of centrifugal force combined with an optical sensor to detect amplification), it would spin samples into independent reaction chambers. This system makes use of a fluorescently labelled RPA assay that can semi-quantitatively determine results. The study showed that the system outperformed PCR chip assays with regards to execution time (under 20 minutes and energy efficiency, while functioning isothermally[15].

2.6 Conclusion

Current diagnostic assays for the detection of both *Candidatus* Phytoplasma asteris and *Coniella granati* are time consuming and require well-equipped diagnostic laboratories. As the diseases caused by these pathogens lead to severe yield losses, it is imperative to find a faster and more efficient detection assay. Recombinase polymerase amplification is an isothermal diagnostic technique that is both fast and efficient and is an ideal candidate to fill this niche. Recombinase polymerase amplification can also be incorporated into a microfluidic device, creating the possibility for lab-free, on-site diagnostic testing, which could be simple enough for a layperson, such as a farmer to use.

Chapter 3 – Materials and Methods

3.1 Introduction

The aim of this study was to develop alternative diagnostic methods, that could be translated into lab-free on-site use. The techniques described in this chapter include symptomology replication, the development of a control construct, isothermal detection assays, comparisons to current diagnostic assays and laying the biological framework for an electronic device, by means of oligonucleotide capture probes.

3.2 Sample acquisition

Candidatus Phytoplasma asteris (AY) DNA positive controls were available from a previous MSc project done in the Vitis Laboratory at Stellenbosch University[6]. These samples were acquired from symptomatic Colombar grapevines from the Vredendal region in the Western Cape, South Africa. DNA from these samples was extracted using the Supaquick CTAB extraction method (Addendum A). These samples were subsequently stored at -20°C until used in this study.

Coniella granati plate cultures were obtained from Ms Elrita Venter at the department of Plant Pathology at Stellenbosch University. These samples were collected and identified from pomegranate sampling trips in the Western Cape pomegranate cultivation region of South Africa. Virulence of these samples were tested by means of Koch's postulates[76]

3.3 Polymerase chain reaction diagnostic assays

A nested-PCR diagnostic assay as described by Van der Vyver[6] was used to confirm the AY phytoplasma status of samples. Primers used in the nested-PCR diagnostic assay are listed in Table 3.1.

Table 3.1 – Primers used for *Candidatus* Phytoplasma asteris nested polymerase chain reaction					
PCR nr	**Primer name**	**Sequence**	**Target**	**Amplicon size (bp)**	**Reference**
1	P1	5' AAG AGT TTG ATC CTG GCT CAG GAT T-3'	16S rDNA	1792	104
	P7	5'-CGT CCT TCA TCG GCT CTT-3'	23S rDNA		105
2	R16F2n	5'-GAA ACG ACT GCT AAG ACT GG-3	16S rDNA	1244	106
	R16R2	5'-TGA CGG GCG GTG TGT ACA AAC CCC G-3'	16S rDNA		107
3	R16(I)F1	5'-TAA AAG ACC TAG CAA TAG G-3'	16S rDNA	1100	107
	R16(I)R1	5'-CAA TCC GAA CTG AGA CTG T-3'	16S rDNA		

Reactions consisted of 0.2 µl of each 20 µM primer (0.2 µM), 0.4 µl of dNTP mix (10 mM)(Thermo Fisher Scientific, MA, United States), 0.16 µl of 5 U KapaTaq DNA Polymerase (1 U)(Kapa Biosystems Inc, Cape Town, South Africa) , 1 µl of 100 ng/µl DNA input, 2 µl of 10X KapaTaq Buffer B with Mg (1X) (Kapa Biosystems Inc, Cape Town, South Africa), 16.04 µl PCR-grade H_2O, making up a final volume of 20 µl. Reaction conditions are listed in Table 3.2. After the respective PCR cycles were completed, 10 µl each were loaded for the first two nested-PCRs, and 20 µl for the third PCR, on separate 1% agarose gels, and stained with EtBr, for visualisation of results.

Table 3.2 - Nested polymerase chain reaction conditions for the amplification of *Candidatus* Phytoplasma asteris 16S rDNA										
Primers	**First hold**		**Cycle 35x**						**Final Hold**	
PCR 1	5'	94°C	Denaturation		Annealing		Elongation		7'	72°C
			30"	94°C	30"	54°C	30"	72°C		
PCR 2	2'	94°C	1'	94°C	2'	58°C	3'	72°C	10'	72°C
PCR 3	2'	94°C	1'	94°C	2'	50°C	3'	72°C	10'	72°C

Primers used in the amplification of *C. granati* were designed from a consensus sequence of *C. granati,* generated in this study. Since the pathogen has undergone multiple name changes, reference sequences from both *Pilidiella granati* and *Coniella granati* were used to construct a consensus sequence. The consensus sequence was created using CLC sequence viewer 8, using the top 15 *ITS1*, 5.8S rRNA and *ITS2* genomic DNA regions available on GenBank. Two PCR primers were designed from

the consensus, namely forward primer PgranatiF1: 5'- AGG ACA CAA CCC CAG ATA CCC -3' and reverse primer PgranatiR1: 5'- ATT CCT ACC TGA TCC GAG GTC -3'. Specificity of the primers were confirmed using NCBI Blast. Primers were also checked using OligoAnalyzer 1.5 to determine that self-annealing and secondary structure properties were not significant.

Crude fungal DNA samples were prepared for PCR by incubating, fungal plugs in 100 µl PCR-grade H_2O at 98°C for 10 minutes. PCR reactions consisted of 1 µl of crude DNA extract, 1 µl of 20 µM of each primer (1 µM) , 0.5 µl dNTP mix (12.5 mM) (Thermo Fisher Scientific, MA, United States), 2.5 µl 10X KapaTaq Buffer A with Mg (1X) (Kapa Biosystems Inc, Cape Town, South Africa), 0.5 µl 25 mM $MgCl_2$ (0.63 mM) (Kapa Biosystems Inc, Cape Town, South Africa), 0.2 µl of 5 U KapaTaq DNA Polymerase (1 U) (Kapa Biosystems Inc, Cape Town, South Africa), 13.3 µl PCR-grade H_2O, making up a final volume of 20 µl. PCR conditions are listed in Table 3.3.

Table 3.3 - Polymerase chain reaction conditions for amplification of *Coniella granati ITS1*, 5.8S rRNA, *ITS2* DNA regions

Primers	**First hold**		**Cycle 35x**						**Final Hold**	
PgranatiF1	5'	94°C	Denaturation		Annealing		Elongation		7'	72°C
PgranatiR1			30"	94°C	30"	54°C	30"	72°C		

PCR products were visualised by agarose gel electrophoresis. Fragments of the expected side were excised, and DNA extracted using a Zymoclean™ gel DNA recovery kit (Zymo Research, CA, United States) and sent for bidirectional Sanger sequencing at the Central Analytical Facility at Stellenbosch University. Sequencing data was evaluated using NCBI Blast.

3.4 AY Control Construct synthesis

An aster yellows control construct (AYCC) was created in order to compare RPA with the existing PCR detection assay. Comparisons included the time required to effectively detect the AYCC, and sensitivity in detecting the AYCC. The AYCC was created by using the product of PCR 2 (of the existing nested PCR), as template to amplify a part of this amplicon, using two mutagenic primers namely, AYConFrag1R1: 5'-AAGGATCCTTTCCATCATTTATTCTTC-3'; and AYConFrag2F2: 5'-

AAGGATCCTTATTGTTAGTTACCAGC-3' (Table 3.4). This resulted in a shortened amplicon, missing the centre portion of the amplicon, as seen in Figure 3.1.

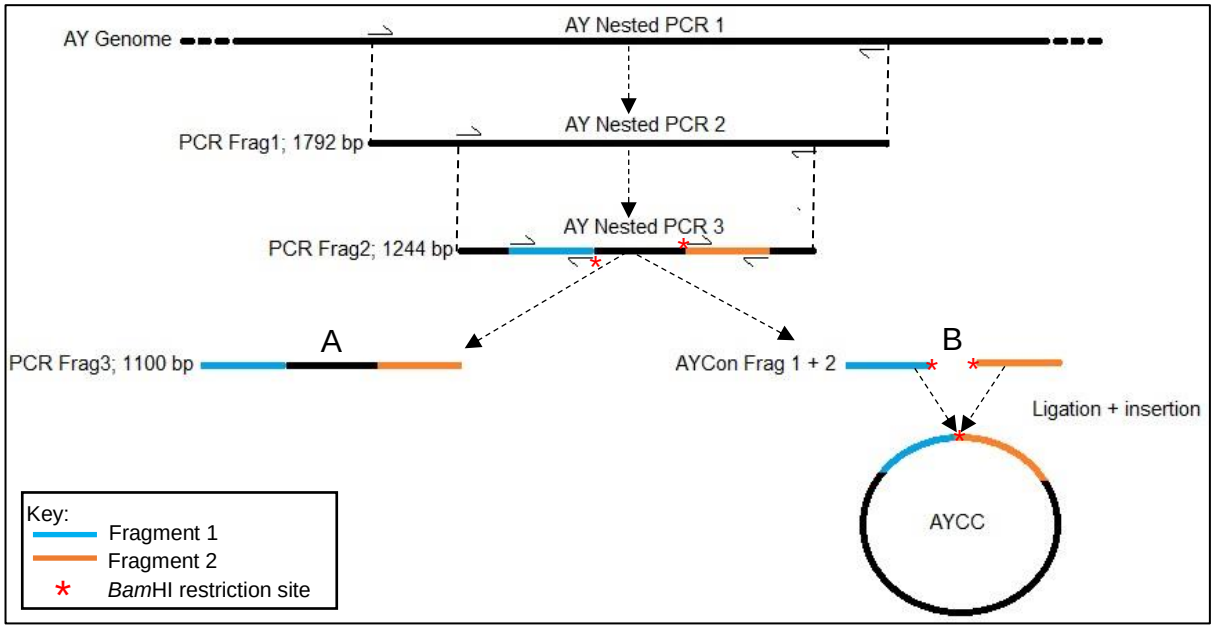

Figure 3.1 -Illustration of the AY nested-PCR protocol (A) and the synthesis of the Aster Yellows Control Construct (B).

In Figure 3.1 A- depicts the normal AY phytoplasma nested-PCR assay, whereas B- depicts the synthesis of the AYCC. Following the protocol for AY nested-PCR 3, as set out in section 3.4, two fragments were amplified, fragment 1 (blue), consisting of forward primer R16(1)F1 and reverse primer AYConFrag1R1 (containing a five prime *Bam*HI restriction site); and fragment 2 (orange) consisting of forward primer AYConFrag1F1(containing a five prime *Bam*HI restriction site) and reverse primer R16(1)R1. The two fragments were excised using the Zymoclean™ gel DNA recovery kit (Zymo Research, CA, United States) and digested together overnight using *Bam*HI at 37°C in a reaction mix consisting of 4 µl of each DNA fragment, 2.5 µl of *Bam*HI digestion buffer (Promega, WI, United States), 12.5 µl of PCR-grade H_2O, and 2 µl of *Bam*HI digestion enzyme (Promega, WI, United States). The insert, consisting of fragment one and fragment two, was then subjected to A-tailing in a reaction mix consisting of 15 µl of the DNA, 0.5 µl of 10 mM ATP (Thermo Fisher Scientific, MA, United States), 2.5 µl of 10X KapaTaq Buffer A with Mg (Kapa Biosystems Inc, Cape Town, South Africa), 0.2 µl KapaTaq DNA Polymerase (Kapa Biosystems Inc, Cape Town, South Africa), and 6.8 µl of PCR-grade H_2O. A tailing was performed in a thermocycler at 72°C for 10 minutes. Once completed, the fragment was ligated into

a Promega pGEM®-T Easy Vector (Promega, WI, United States) at 4°C overnight in a reaction mix consisting of 2 µl of 2X ligation buffer, 1 µl of pGEM®-T Easy Vector (Promega, WI, United States), 1 µl of Promega T4 DNA ligase (Promega, WI, United States), and 3 µl of the DNA fragment. The AYCC was then transformed into *Escherichia coli* strain JM109 and plated onto selective Luria-Bertani (LB) media containing 100 µg/ml Ampicillin, 80 µg/ml 5-Bromo-4-Chloro-3-Indolyl β-D-Galactopyranoside (X-gal) (Thermo Fisher Scientific, MA, United States), and 0.5 mM isopropyl β-D-1-thiogalactopyranoside (IPTG) (Thermo Fisher Scientific, MA, United States). Selective plates were incubated at 37°C overnight. Thirty-two white colonies were selected for colony PCR to confirm that the fragments were inserted in the correct orientation, this was performed using PCR 3 primers as listed in Table 3.1. PCR products were visualised on a 1% agarose gel, stained with EtBr. Of the 32 colonies, 4 were selected, and their plasmids extracted using Qiagen QIAprep Spin Miniprep Kit (Qiagen, Venlo, Netherlands). Inserts were digested using *Eco*RI in a reaction mix containing 10 µl of PCR-grade water, 7 µl of the plasmid DNA, 2 µl of *Eco*RI digestion buffer (Thermo Fisher Scientific, MA, United States) and 1 µl of *Eco*RI digestion enzyme (Thermo Fisher Scientific, MA, United States). Digestion was performed at 37°C for two hours, after which digested inserts were visualised on a 1% agarose gel, stained with EtBr. The AYCCs extracted from the 4 selected colonies were sent for bidirectional Sanger sequencing at the Central Analytical Facility (CAF) at Stellenbosch University using SP6 and T7 promotor primers supplied by CAF. Sanger sequence data was analysed using CLC sequence viewer 8 and compared to the *in-silico* version of the control construct sequence, available in Addendum B. The four selected *E. coli* colonies were grown in LB broth overnight and 50% glycerol stocks were made, and stored at -80°C.

3.5 RPA diagnostic assays

Primers for three RPA diagnostic assays, AYCC, AY phytoplasma and *C*. *granati* were designed according to the specifications of the TwistDX® Basic kit (TwistDx, Cambridge, United Kingdom)[93]. Primers were approximately 30 bases long, had at least 50% GC content and a GC-rich 3’ end. Primers were designed according to the AY PCR 3 consensus sequence. The specificity of these primers was determined using NCBI Blast, and OligoAnalyzer 1.5 was used to determine that self-annealing

and secondary structures were insignificant. Primers used for both RPA diagnostic tests are listed in Table 3.4.

Table 3.4 - Primers: Aster Yellows control construct, *Candidatus* Phytoplasma asteris and *Coniella granati* recombinase polymerase amplification

RPA Diagnostic	Primer name	Sequence	Target	Amplicon size (bp)
AYCC RPA	AYConRPAF1	5'-TAG CAA TAG GTA TGC TTA GGA GGA GCT TGC G -3'	AYCC	450
	AYConRPAR1	5'- CCG AAC TGA GAC TGT TTT TTT GAG ATT CGC -3'	AYCC	
AY RPA	AY16SRPAF	5'- AAA AAC TGT TTA GCT AGA GTA AGA TAG AGG -3'	16S rDNA	370
	AY16SRPAR	5'-TAC AGC TTT GCA GAA GCA TGT CAA GAC CTG G -3'	16S rDNA	
C. granati RPA	PgranatiRPAF1	5'- ATA TCG TTG CCT CGG CGC TGA GCT GGG GGC -3'	*ITS1*, 5.8S rRNA and *ITS2*	470
	PgranatiRPAR1	5'- ATT GGT GGG GTT TTA CGG CAA GAG CAC CGC -3'	*ITS1*, 5.8S rRNA and *ITS2*	470

Sensitivity of the RPA diagnostic was tested by means of a dilution series of AYCC, ranging from 100 ng/µl to 0,1 fg/µl, with concentrations decreasing in 10-fold increments. The dilution series was done to a point of theoretical zero copies of DNA in solution using the formula: number of copies in solution = (amount input DNA (ng) x 6.022×10^{23}) / (estimated length of DNA (bp) x 1×10^{9} x 650 (Da))[104]. RPA and PCR diagnostics were run using the dilution series, as described above. The PCR mix is described in section 3.4, with the only alteration being that 1.2 µl of the diluted AYCC DNA was added. PCR conditions were the same as PCR 3 of the nested-PCR diagnostic, as seen in Table 3.4. RPA reactions consisted of 1 freeze-dried solution pellet (supplied in the kit), consisting of a patented recipe of dNTPs, single stranded binding proteins (SSBs), recombinase, and polymerase, 2.4 µl of 10 µM of each primer (Table 3.4), 29.5 µl rehydration buffer (supplied in the kit), 1.2 µl of AYCC DNA dilutions, 12 µl PCR-grade H_2O, and 2.5 µl of 280 mM MgOAc (supplied in the kit), making up a final volume of 50 µl. RPA reactions were incubated at 37.5°C for 40 minutes with intermittent mixing using a Vortex Genie 2 every 10 minutes, to increase sensitivity. After incubation, reactions were terminated by incubating at 65°C for 10 minutes, to dissociate DNA binding proteins[11]. Amplified DNA fragments were visualised on a 1% agarose gel, stained with EtBr. This experiment was repeated three times to evaluate the consistency of the diagnostic assays.

The next comparison consisted of a time test that was performed by incubating the AYCC RPA reaction mix at 37.5°C and incrementally (every 10 minutes), removing the tubes from incubation and placing them on ice at -20°C. By placing the RPA reactions on ice, it effectively stopped any amplification from progressing. This was done every 10 minutes for an hour. After the final tube was removed and placed on ice, all tubes were then incubated at 65°C for 10 minutes to dissociate DNA binding proteins. Once incubation was done, 20 µl of each solution was subjected to agarose gel electrophoresis. This experiment was repeated twice, to evaluate the consistency of the results.

RPA reactions for the detection of *Candidatus* Phytoplasma asteris and *Coniella granati* consisted of 1 freeze dried solution pellet (supplied in the kit), 2.4 µl of 10 µM of each primer (Table 3.4), 29.5 µl rehydration buffer (supplied in the kit), 1 µl of extracted/crude DNA, 12.2 µl PCR-grade H_2O, 2.5 µl of 280 mM MgOAc (supplied in the kit), making up a final volume of 50 µl. Similar to the AYCC RPA diagnostic, the RPA diagnostic reactions were incubated at 37.5°C for 40 minutes, mixing by means of a Vortex Genie 2 every 10 minutes, after which the reactions were incubated at 65°C for 10 minutes to dissociate DNA binding proteins. Twenty microliters of the reaction were visualised by agarose gel electrophoresis. For the AY RPA diagnostic, fragments of the expected size were then excised from the gel and DNA extracted using a Zymoclean™ gel DNA recovery kit (Zymo Research, CA, United States). DNA samples were sent for bidirectional Sanger sequencing at the Central Analytical Facility at Stellenbosch University. Sequencing data was evaluated using NCBI Blast and can be seen in Addendum C.

3.6 Use of biotinylated oligonucleotide probes to capture amplified DNA

Biotinylated oligonucleotide capture probes for the microfluidic device were designed to be specific to each organism being tested for. These probes were subjected to specificity tests using streptavidin-coated magnetic beads.

Three biotinylated oligonucleotide capture probes were designed, to hybridise to the *Candidatus* Phytoplasma asteris RPA amplicon. Two probes (probes 1 & 3) were designed to capture the positive sense and one (probe 2) to capture the negative sense strand. This is illustrated in Figure 3.2.

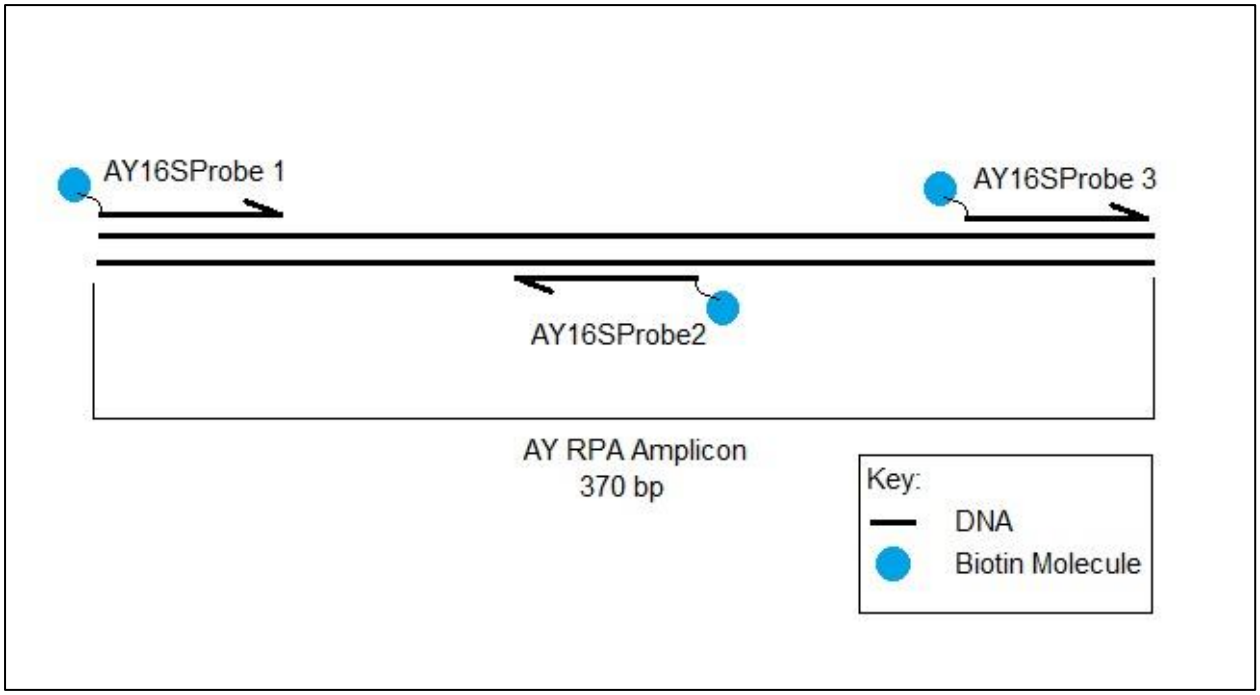

Figure 3.2 - Illustration of biotinylated oligonucleotide capture probes hybridising to the *Candidatus* Phytoplasma asteris recombinase polymerase amplification product.

Table 3.5 contains the sequences of AY phytoplasma biotinylated probes. Specificity of the probes were tested using NCBI Blast, whereas OligoAnalyzer 1.5 was used to determine that the self-annealing properties of the probes were insignificant.

Table 3.5 - *Candidatus* Phytoplasma asteris biotinylated oligonucleotide capture probes

Probe name	**Sequence**	**Target**
AY16SProbe1	5'-/5Biosg/CAT GTG TAG TGG TAA AAT GCG TAA ATA TAT -3'	16S rDNA
AY16SProbe2	5'-/5Biosg/CGT TTA GTA CTC ATC GTT TAC GGC GTG GAC -3'	16S rDNA
AY16SProbe3	5'-/5Biosg/GCA CAA GCG GTG GAT CAT GTT GTT TAA TTC -3'	16S rDNA

In order to detect *C*. *granati* RPA amplicons, four biotinylated oligonucleotide capture probes of 30 nucleotides each were designed. Two of these probes (1 & 3) were designed to hybridise with the positive strand of putative RPA amplicons, and two (2 & 4) to hybridise with the negative sense strand. Figure 3.3 illustrates the hybridisation of biotinylated oligonucleotide capture probes hybridising to specific locations on the *C*. *granati* RPA amplicon.

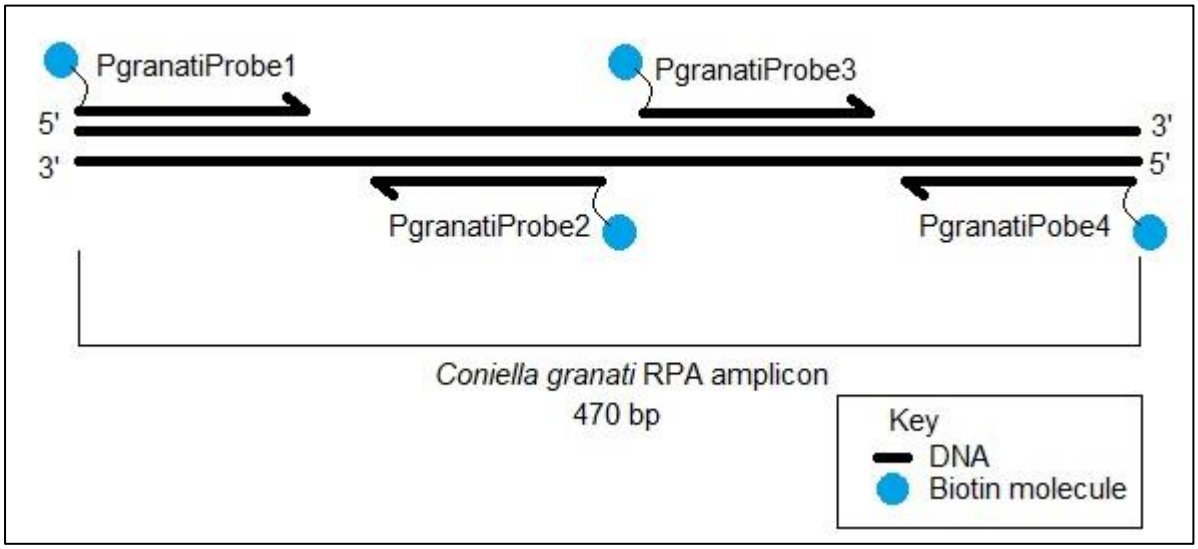

Figure 3.3 - Illustration of the hybridisation sites of biotinylated oligonucleotide capture probes hybridising to the *Coniella granati* recombinase polymerase amplification amplicon.

Table 3.6 below contains the sequences of all four *C. granati* biotinylated probes. Specificity of the probes was tested using NCBI Blast, whereas OligoAnalyzer 1.5 was used to determine that the self-annealing properties of the probes were insignificant.

Table 3.6 - Probes: *Coniella granati* biotinylated oligonucleotide capture probes

Probe name	**Sequence**	**Target**
Pgranati Probe1	5'-/5Biosg/TCT TTC CAA GAA GCT CTC CCA TGG TCT CTC -3'	*ITS1*, 5.8S rRNA and *ITS2*
Pgranati Probe2	5'-/5Biosg/TTT TGA TTC ATT TTG TTT TGA ATA ACT CAG -3'	*ITS1*, 5.8S rRNA and *ITS2*
Pgranati Probe3	5'-/5Biosg/CGA GCG TCA TTT CAC CCC TCA AGC CTT GCT -3'	*ITS1*, 5.8S rRNA and *ITS2*
Pgranati Probe4	5'-/5Biosg/CTT CCA AAG CGA GGT GAT AAA CTA CTA CGC -3'	*ITS1*, 5.8S rRNA and *ITS2*

Streptavidin-coated magnetic beads (Thermo Fisher Scientific, MA, United States) were used to assess the ability of probes to capture RPA amplified AY phytoplasma and *C. granati* DNA. One microliter of each probe (20 µM) was added to the RPA amplicon, denatured for 10 minutes at 95°C, and then immediately cooled and renatured on ice for 2 minutes. The "Streptavidin-Coated Microspheres Binding Biotinylated DNA" protocol (Polysciences, Inc., PA, United States) was followed to capture amplified DNA using streptavidin-coated magnetic beads[105], however only half

the specified amount of streptavidin-coated microspheres was used. Fifty microliters of streptavidin-coated magnetic beads were washed twice with 100 µl binding and wash (B&W) buffer, centrifuged at 10 000 rpm for 3 minutes, decanting the supernatant between washes. Washed magnetic beads were then resuspended in 20 µl of B&W buffer. Fifty microliters of the DNA-probe solution were then added to the resuspended magnetic beads, and vortexed for 15 minutes at room temperature, on a Vortex Genie 2. Beads were washed two more times, using B&W buffer, as described before. DNA was recovered from the magnetic beads by adding 150 µl of 0.2 M NaOH and vortexed for 6 minutes at room temperature, on the lowest setting of a Vortex Genie 2 shaker. Fifty microliters of captured DNA were then viewed on a 1% agarose gel, stained with EtBr. Biotinylated probes were stripped from the streptavidin magnetic beads by resuspension in PCR-grade H_2O and then incubated at 70°C for 20 minutes, and the beads subsequently concentrated using a magnet. Washed streptavidin magnetic beads were then stored at 4°C for future use.

Chapter 4 – Results and Discussion

4.1 Polymerase chain reaction diagnostic assays

Current diagnostic protocols for the detection of AY phytoplasma comprises of a nested-PCR approach that consists of three consecutive PCRs, as described by van der Vyver[6]. The problem with this approach is that it takes more than 10 hours to complete, 1h 40 minutes for PCR 1, 4 hours for PCR 2, and 4 hours for PCR 3, plus another 40 minutes for gel electrophoresis and visualisation. Occasionally results can be visualised at the end of PCR 2, however in most cases all three nested-PCRs must be completed before results can be assessed, this is due to the low titre of the pathogen present in the plant. AY phytoplasma nested-PCR results can be seen in Figures 4.1-4.3. A limitation of the nested-PCR process is that it is time consuming and labour intensive.

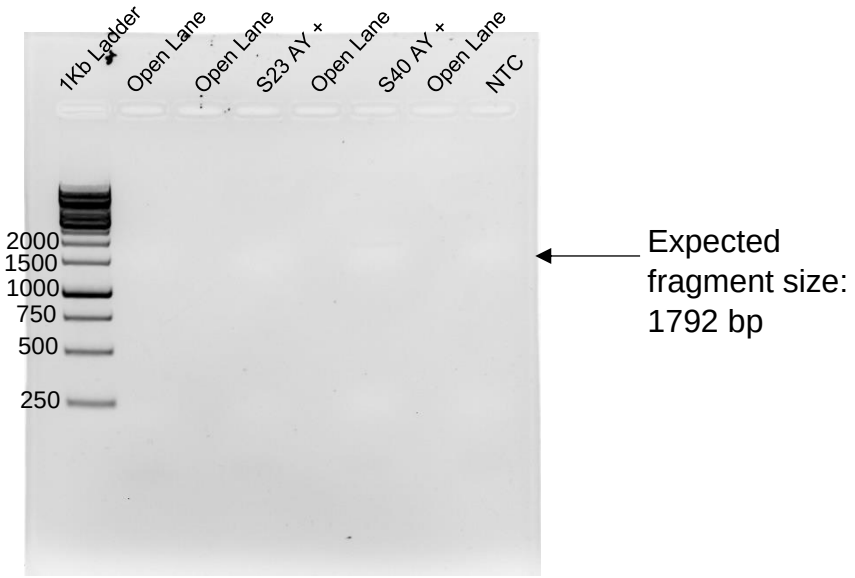

Figure 4.1 - *Candidatus* Phytoplasma asteris nested polymerase chain reaction 1, on 1% agarose gel. Lane 1: GeneRuler™1kb DNA Ladder; Lane 2: Open lane; Lane 3: Open Lane; Lane 4: Aster Yellows Positive control (S23); Lane 5: Open Lane; Lane 6: Aster Yellows Positive control (S40); Lane 7: Open Lane; Lane 8: No-template Control.

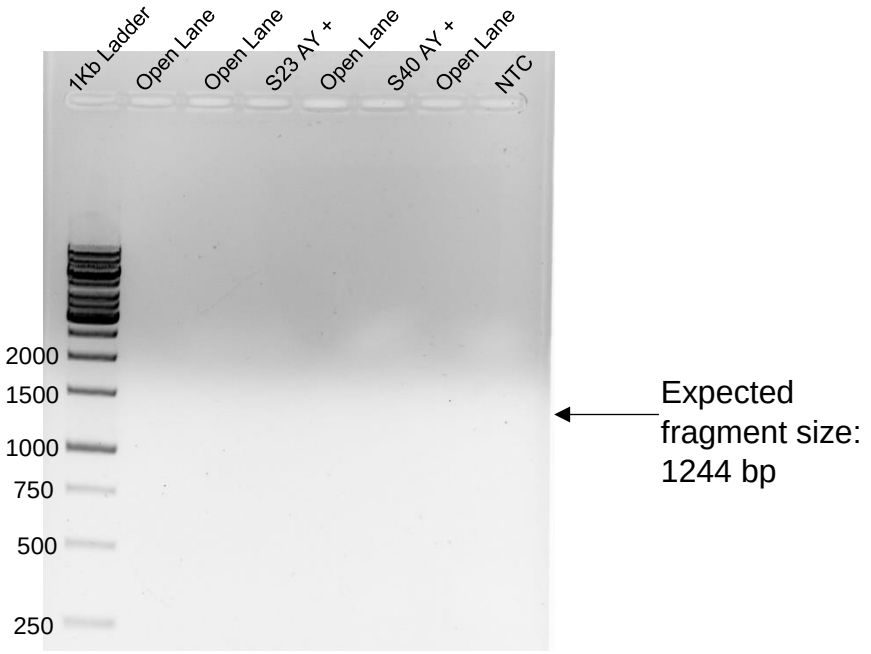

Figure 4.2 - Candidatus Phytoplasma asteris nested polymerase chain reaction 2, on 1% agarose gel**.** Lane 1: GeneRuler™1kb DNA Ladder; Lane 2: Open lane; Lane 3: Open Lane; Lane 4: Aster Yellows Positive control (S23); Lane 5: Open Lane; Lane 6: Aster Yellows Positive control (S40); Lane 7: Open Lane; Lane 8: No-template Control.

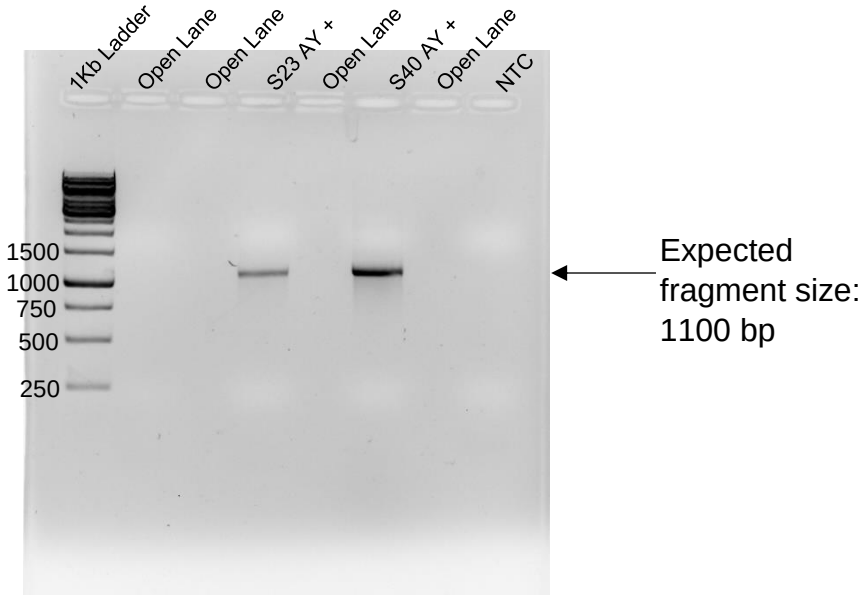

Figure 4.3- *Candidatus* Phytoplasma asteris nested polymerase chain reaction 3, on 1% agarose gel. Lane 1: GeneRuler™1kb DNA Ladder; Lane 2: Open lane; Lane 3: Open Lane; Lane 4: Aster Yellows Positive control (S23); Lane 5: Open Lane; Lane 6: Aster Yellows Positive control (S40); Lane 7: Open Lane; Lane 8: No-template Control.

PCR and RPA diagnostic assays for the detection of *C*. *granati* were designed taking future lab-free, on-site use into consideration. Therefore, the DNA for both diagnostic assays consisted of crudely extracted fungal DNA. An observation made when taking this approach was that plugs selected from the outer extremities of the fungal colony were more likely to result in a false negative in both PCR or RPA diagnostics. Whereas, plugs that selected from the centre of the colony were consistently detected by both diagnostic assays. This might be due to the overlapping nature of the fungal colony, the second layer overlapping the first, where the centre of the colony consists of multiple layers and the outer extremity only consisting of a single layer. The centre of the colony, therefore, probably consists of more cells and subsequently, possibly has higher concentrations of DNA. A limitation, during this thesis, was that no symptomatic plants were available for diagnostic tests of both the PCR and RPA assays, thus colonies were diluted in H_2O as well as in pomegranate juice. Pomegranate juice was used to simulate the natural circumstances in which the fungus would occur; this was a way to test the interaction of phenolic compounds in the juice and the diagnostic assays.

Coniella granati PCR diagnostics results can be seen in Figure 4.4, indicating the successful detection of *C*. *granati*, suggesting that a nested-PCR approach, as suggested in literature[9], is not required when using plate cultures as opposed to infected fruits. The time required to detect *C*. *granati* using PCR was 1h 40min, plus an additional 40 minutes for visualisation by gel electrophoresis. As seen in lanes 3 and 4, the PCR diagnostic worked for both H_2O and juice controls. As no positive control for the PCR was available, amplicons were excised, and DNA extracted from the excised bands was sent for bidirectional Sanger sequencing. Sequences were aligned and trimmed using CLC sequence viewer 8. A consensus sequence was generated and subjected to NCBI Blast analysis. The blast revealed 99% identity (E-value of 0) to that of *C*. *granati* and *P*. *granati*. This sequence can be viewed in Addendum D.

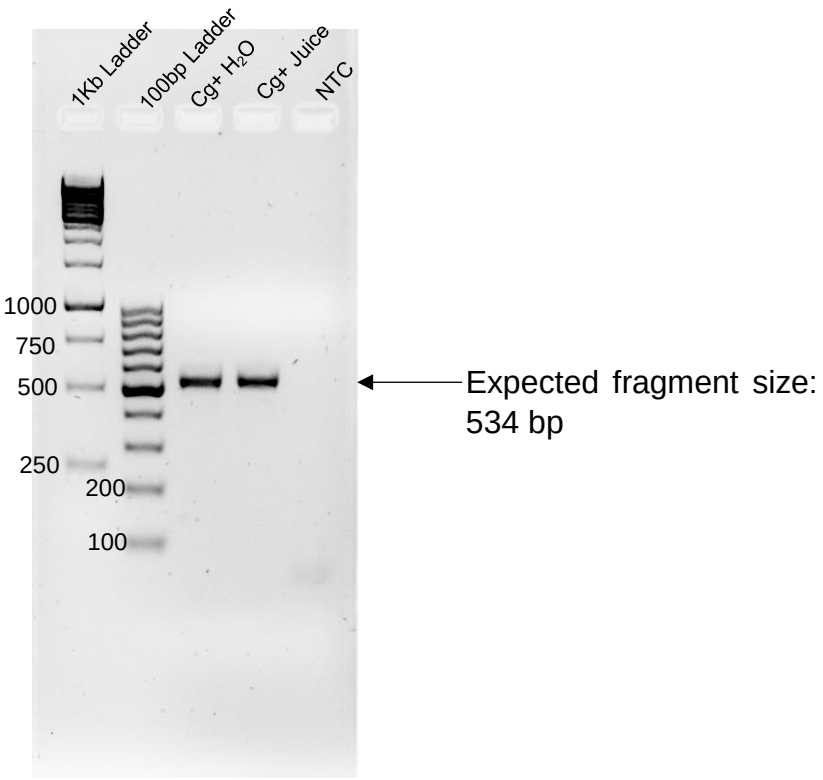

Figure 4.4 - *Coniella granati* polymerase chain reaction, on 1% agarose gel. Lane 1: GeneRuler™1kb DNA Ladder; Lane 2: O'GeneRuler™ 100 bp DNA ladder; Lane 3: *Coniella granati* positive control in H_2O; Lane 4: *Coniella granati* positive control in Juice; Lane 5: No template control

4.2 Comparison between RPA and PCR

The AY control construct (AYCC), as described in Chapter 3, section 3.4 was created for three reasons; firstly, it allowed positive control DNA to be readily available, at high concentrations. This circumvents the need for naturally occurring AY DNA, which tends to only be present at low concentrations in plants. Aster yellows DNA concentrations are impossible to discern from that of the plant DNA, once extracted, meaning that accurate sensitivity comparisons could not be done. The AYCC therefore, allowed for precise control construct DNA concentrations to be determined. The second reason for the AYCC was that it consisted of AY DNA with recognisable primer regions, for which primers had already been designed, see PCR 3 primers in Table 3.1. The third reason is that the modification of the fragment both shortened the amplicon fragment and introduced a restriction site (*Bam*HI) in the centre of the new fragment.

The AYCC DNA fragment was modified from its naturally occurring counterpart, as isothermal amplification techniques have been known to amplify at room temperature increasing the risk of contamination in future experiments. Therefore, if contamination should have occurred, amplicons in diagnostic assays would be shorter than expected and could be digested using the *Bam*HI digestion enzyme to determine the source of the contaminants. Thus, the AYCC could be ideally used to test and verify conclusions made in literature[98], such as time and sensitivity tests, between PCR and RPA diagnostic assays.

Comparison tests were done between PCRs and RPAs using the AYCC, these tests included a sensitivity and time test. Sensitivity test results can be seen in Table 4.1.

Table 4.1 - Detection specificity results of PCR vs RPA using AYCC

Starting Concentration ng/µl	**Volume added µl**	**Final Concentration ng/µl**	**Theoretical copies of DNA**	**Detected**	
				PCR	**RPA**
85	1.2	100	26470329670	✓	✓
8.5	1.2	10	2699973626	✓	✓
0.85	1.2	1	269997363	✓	✓
0.085	1.2	0.1	26999736	✓	✓
0.0085	1.2	0.01	2699974	✓	✓
0.00085	1.2	0.001	269997	✓	✓
0.000085	1.2	0.0001	27000	✓	✓
0.0000085	1.2	0.00001	2700	✓	✓
0.00000085	1.2	0.000001	270	✓	✓
0.000000085	1.2	0.0000001	27	✓	X
0.0000000085	1.2	0.00000001	3	X	X
0.00000000085	1.2	0.000000001	0	X	X

Time test analyses of RPA indicated that the RPA diagnostic assay could accurately detect AYCC at a concentration of 1 fg/µl, in 20 minutes, this can be broken down into 10 minutes of amplification at 37.5°C and 10 minutes of protein dissociation at 65°C. However, these results had to be visualised on an agarose gel that ran for 40 minutes at 100V. PCRs consistently performed better than the RPA, with regards to sensitivity, by a ten-fold margin, similar to studies done by Lau *et al.* [96] and Rojas *et al*.[98]. As the AYCC is extracted from *E*. *coli*, certain cellular components may still be present in the extract. These components may have interfered with the sensitivity of the RPA

diagnostic assay as compared to the PCR, as clearly stated by the manufacturer[93]. When assessing time tests, the RPA assay dramatically outperformed those of the PCR assay. RPA diagnostic results could be ascertained in an hour from start of the diagnostic to visualisation of the results, whereas the PCR assays required a minimum of two and a half hours to complete. This further verified the conclusions made in previous diagnostic studies, that although PCR diagnostic assays were more sensitive than those of the RPA assays, that the RPA diagnostics were significantly faster at determining a result[13,97,98].

4.3 Recombinase polymerase amplification diagnostics assays

The AY RPA diagnostic test, as seen in Figure 4.5, was done with multiple controls to ensure specificity and sensitivity. These controls include the RPA positive control (supplied with the kit), a negative control (*Vitis vinifera* DNA), and a no-template control. The RPA positive control was used to ensure that the RPA reagents and enzymes functioned as it should. The *V. vinifera* negative control was used to ensure that nothing within the plant was reacting with the diagnostic test and giving false positive results. The No-template control was used to ensure that no contamination occurred. The positive controls used in the diagnostic included AY positive DNA diluted in both water and grape juice. The reason for the dilution in juice was to ensure that plant phenolics did not entirely impede the RPA diagnostic.

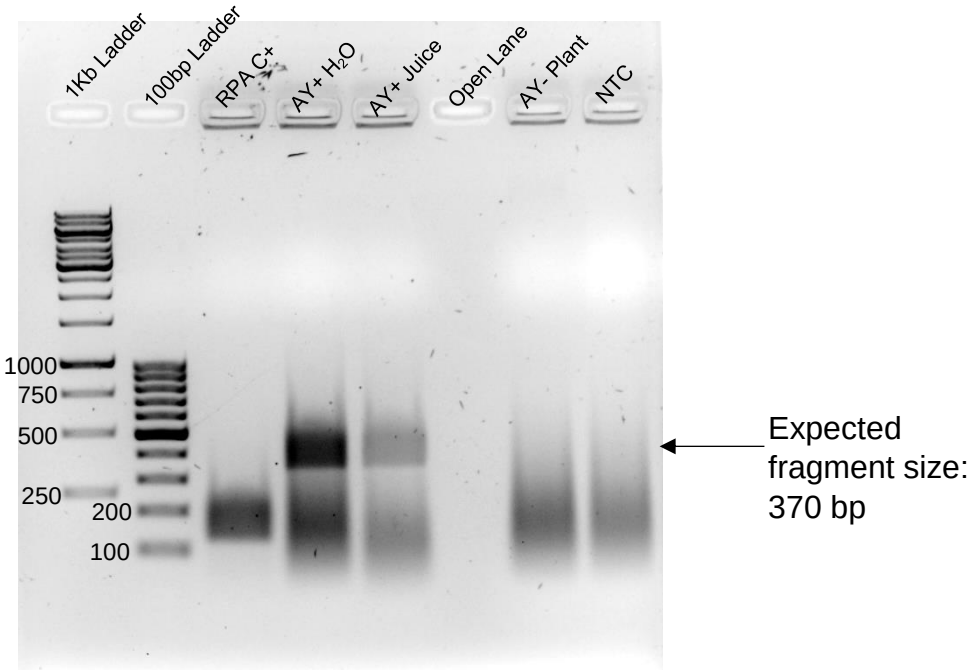

Figure 4.5 - *Candidatus* Phytoplasma asteris recombinase polymerase amplification, on 1% agarose gel. Lane 1: GeneRuler™1kb DNA Ladder; Lane 2: O'GeneRuler™ 100 bp DNA ladder; Lane 3: RPA positive control; Lane 4: *Candidatus* Phytoplasma asteris in H2O; Lane 5: *Candidatus* Phytoplasma asteris positive in pomegranate juice; Lane 6: open lane; Lane 7: Negative control (*Vitis vinifera*); Lane 8: No-template control

Positive plant material would have been ideal, however due to the excessive drought conditions experienced in the Western Cape, it has been observed that grapevines have gone into a hypothesised form of remission similar to a recovery phenotype[6]. It appears that juice influences the RPA diagnostic, this is a reason for concern, as plant phenolics might inhibit the specificity of the diagnostic.

The RPA diagnostic assay proved highly effective at detecting *C*. *granati* working at a constant temperature of 38°C, with first results available in 30 minutes, however the optimal incubation time proved to be 40 minutes. Intermittent mixing resulted in more effective results; similar to the AY phytoplasma RPA diagnostic. To test the specificity of the RPA diagnostic a negative control was included, namely *Aureobasidium pullulans*, a fungal endophyte known to colonise different plant species. *A*. *pullulans* was chosen because of its abundance and because it is an opportunistic plant fungus found on the pomegranate fruits. As seen in Figure 4.6, only reactions containing *C*. *granati* generated amplicons, whereas the reaction containing *A*. *pullulans* did not. This indicates that the RPA diagnostic is specific enough for detection of *C*. *granati* in

relation to another plant fungus, found in the same fruit. In future studies negative controls within the genus *Coniella* should be tested to ascertain the complete specificity of the diagnostic test, because *In silico* specificity tests do not necessarily relate to *In vitro* results. It is thus imperative that more samples from the genus *Coniella* be tested.

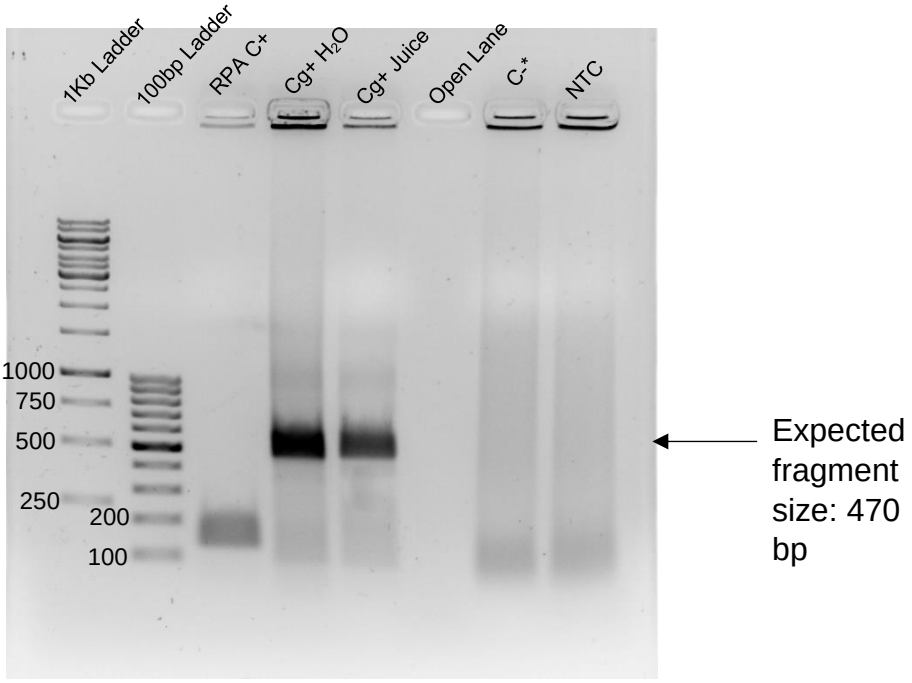

Figure 4.6- *Coniella granati* recombinase polymerase amplification, on 1% agarose gel. Lane 1: GeneRuler™1kb DNA Ladder; Lane 2: O'GeneRuler™ 100 bp DNA ladder; Lane 3: RPA positive control; Lane 4: *Coniella granati* positive in H_2O; Lane 5: *Coniella granati* positive in pomegranate juice; Lane 6: open lane; Lane 7: Negative control (*Aureobasidium pullulans*); Lane 8: No template control

RPA diagnostic products in this chapter were cleaned of single-stranded binding proteins by means of dissociation at 65°C for ten minutes. This was done as SSBs cause smearing and inconsistent band sizes on an agarose gel. Alternative methods for cleaning RPA amplicons exist e.g. Qiagen QIAquick columns, incubation for 10 minutes at 95°C, mini-phenol/chloroform treatment, or 10% SDS treatment, and should be investigated in future studies[11]. These methods should be explored to determine the most efficient method, both time and cost related, of cleaning RPA amplicons.

An observation regarding the kit was that freeze-dried reagents were supplied in the TwistDx® Basic kit (TwistDx, Cambridge, United Kingdom) in eight-unit strip tubes. The lids of these strip tubes tend to open when incubated, increasing exposure and risk to contamination, between adjacent tubes. This problem was solved by transferring the freeze-dried reagents to sealable single-unit Eppendorf.

The RPA diagnostic test for the detection of AY phytoplasma was more sensitive than that of the PCR, reducing the detection time from ten hours, using the nested-PCR approach to an hour and a half, using the RPA approach. Similarly, the detection of *C. granati* was half that of the PCR when using RPA. The time efficiency is a benefit to diagnostic laboratories, as the time required to detect pathogens is significantly decreased when using an RPA detection method.

4.4 Oligonucleotide capture probes

Although the RPA diagnostic assays are already faster than their PCR counterparts, it is still not entirely viable for on-site use, as results still need to be visualised on an agarose gel. Multiple solutions have been developed to address this. Most methods make use of biotin-antibody or biotin-streptavidin interactivity. One solution is to develop a method which combines RPA with a microfluidic or electronic device.

In this thesis, novel biotinylated oligonucleotide probes were used to capture (by hybridisation) pathogen-specific RPA amplicons, with the aim of eventually binding these probes to an electronic device. Biotinylated oligonucleotide capture probes were designed to hybridise to the RPA amplicons, as seen in section 3.6. For the AY phytoplasma RPA diagnostic, three such capture probes were designed and for the *C. granati* RPA diagnostic, four were designed.

Figure 4.7 A – illustrates the route used to test the specificity of the oligonucleotide probes in this study. The probes were tested for specificity using streptavidin magnetic beads/microspheres (Thermo Fisher Scientific, MA, United States). Since biotin and streptavidin form very strong non-covalent bonds, biotinylated probes that hybridise to the RPA amplicon will bind to the streptavidin-coated beads. Probes were tested against different control groups to ensure pathogen specificity. This was done by hybridising probes and RPA amplicons by means of rapid boiling and immediate cooling on an ice slurry. This process was done to enable single stranded

oligonucleotide capture probes, containing a biotin molecule, to attach to their complementary dsDNA amplicon. Biotinylated oligonucleotide-amplicon complexes could now be captured using streptavidin-coated magnetic beads. Multiple wash steps ensured that any unbound DNA was washed away and only those attached to the microspheres remained. Attached DNA was chemically separated from the probes using diluted NaOH, after which it was visualised following agarose gel electrophoresis. Results of this experiment can be viewed in Figures 4.8 and 4.9.

Route B in Figure 4.7 illustrates an alternative method of specificity tests for the oligonucleotide capture probes. In this method, biotinylated probes are bound to the streptavidin-coated microspheres first, and then allowing hybridisation between the probe-bead complex and the single-stranded RPA amplicons. This would be determining whether effective capturing of DNA takes place if probes are directly attached to the streptavidin-coated microspheres and then hybridised to the denatured RPA amplicons. This method would determine whether probes already attached to the microspheres interact with each other and cause non-specific binding, resulting in suboptimal capturing of dsDNA amplicons and/or false negative results. A further reason to explore this method is to determine the capturing potential of probes attached to the microspheres and compare those results with the capturing potential of unattached probes. This would determine which route would optimal for use in a microfluidic device.

Oligonucleotide capture probes can also be attached to a streptavidin-coated electronic device, as seen in route C of Figure 4.7. At every step in the process a baseline current is measured. Once oligonucleotide capture probes have been attached to the electronic device, a working baseline current is determined. Once the pathogen-specific amplicons are washed across the surface of the electronic device the probes will attach to complementary DNA fragments causing a current differential change, indicating positive interaction i.e. a positive diagnostic. This device is currently being developed by the department of Electronic and Electrical Engineering at Stellenbosch University.

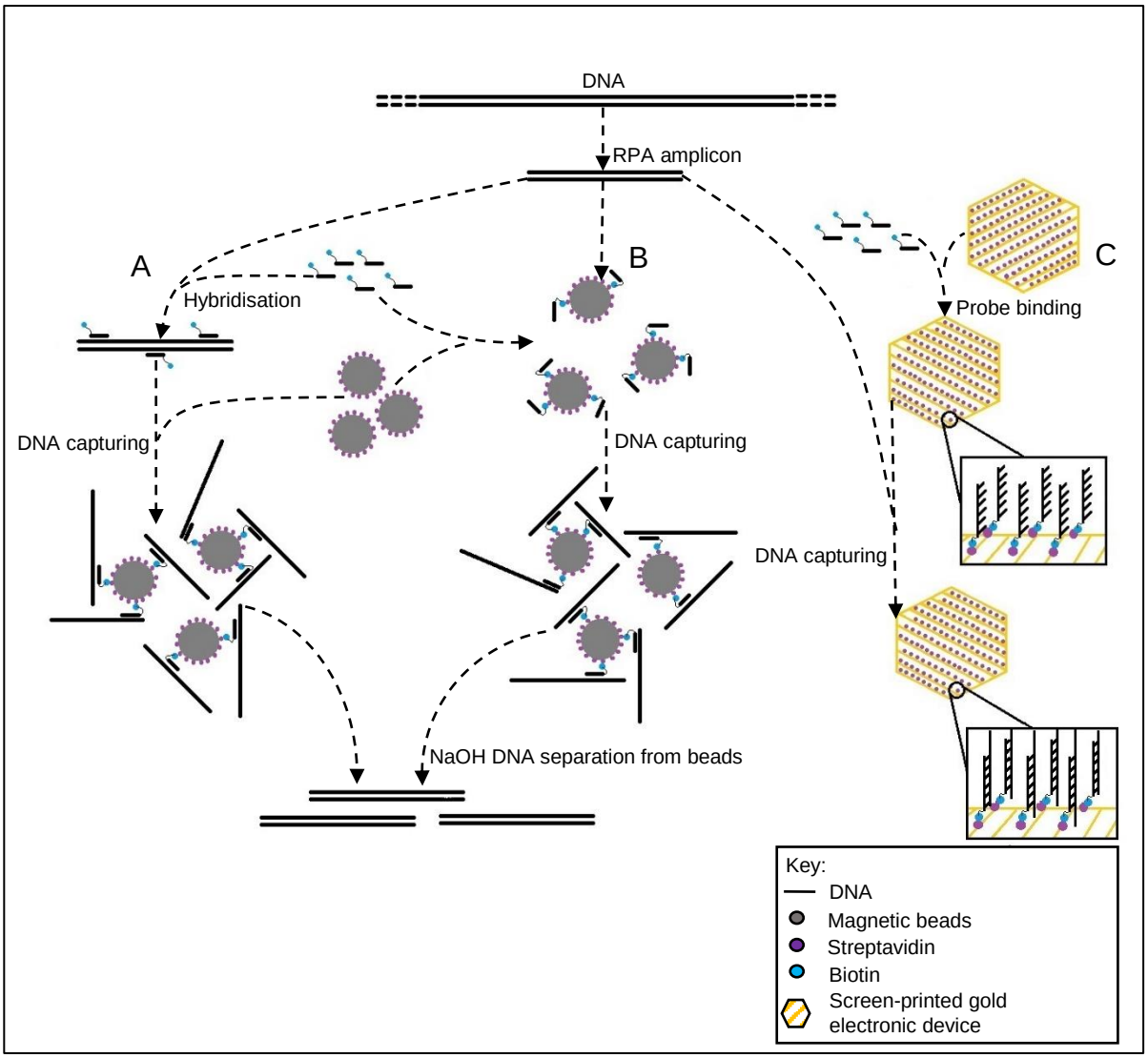

Figure 4.7 – Illustration of three methods of DNA amplicon capture routes. A – depicting the method used in this thesis to test specificity of probes. B – depicting alternative method of DNA capturing. C- depicting electronic device method employed by the Department of Electronic and Electrical Engineering.

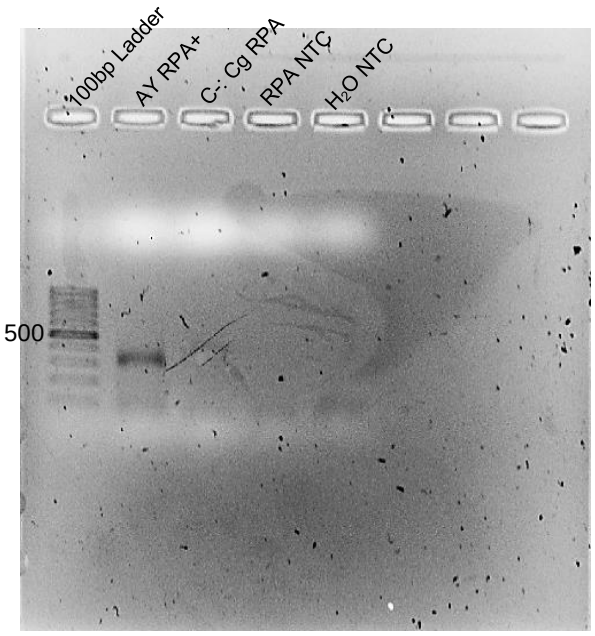

Figure 4.8 - *Candidatus* Phytoplasma asteris recombinase polymerase amplification streptavidin-biotin probe interaction test (Magnetic Streptavidin beads test), on 1% agarose gel. Lane 1: O'GeneRuler™ 100 bp DNA ladder; Lane 2: *Candidatus* Phytoplasma asteris positive DNA; Lane 3: Negative control (*Coniella granati*); Lane 4: RPA no-template control; Lane 5: H_2O no-template control.

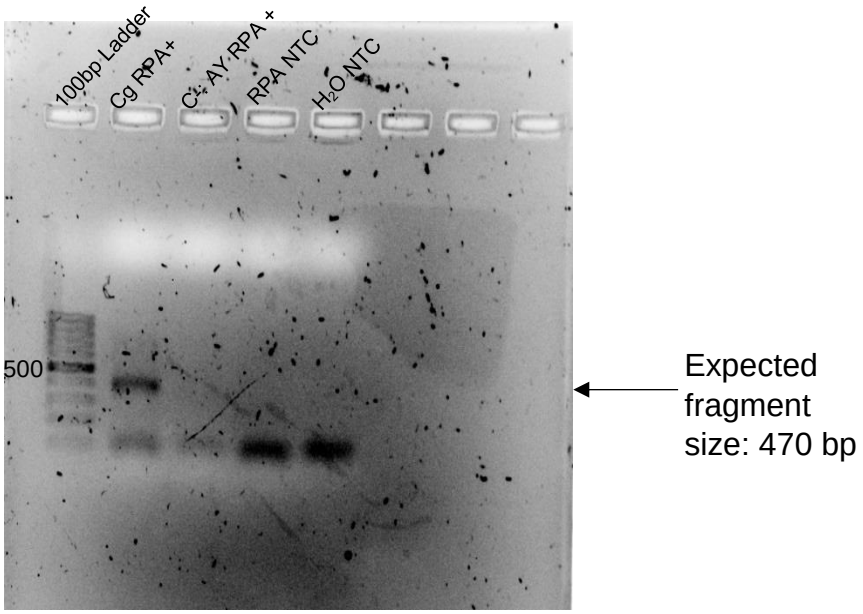

Figure 4.9- *Coniella granati* recombinase polymerase amplification streptavidin-biotin probe interaction test (Magnetic Streptavidin beads test), on 1% agarose gel. Lane 1: O'GeneRuler™ 100 bp DNA ladder; Lane 2: *Coniella granati* positive DNA; Lane 3: Negative control (*Candidatus* Phytoplasma asteris); Lane 4: RPA no template control; Lane 5: H_2O no-template control.

For the AY phytoplasma RPA probe specificity test, Figure 4.8, three negative controls were used to test the specificity of the probes, these included a *Coniella granati* RPA amplicon as a negative control, a no-template control consisting of only RPA reagents, and a no-template control consisting of water. The *C*. *granati* negative control was used to determine that the specificity of the AY phytoplasma capture probes and that no nonspecific hybridisation takes place. The RPA NTC was used to determine that the AY probes do not hybridise to any of the RPA reagents present during amplification, and the water NTC was used to determine that the probes do not self-anneal. As can be seen in Figure 4.8 probes only hybridised to AY RPA amplicons.

For the *C*. *granati* RPA probe specificity test, Figure 4.9, three negative controls were again used; however, an AY phytoplasma RPA amplicon was used as a negative control along with the same RPA NTC and water NTC. As seen in Figure 4.9 probes only hybridised with complementary DNA and did not interact with the reaction mix or unrelated DNA products. In all lanes, but especially in lanes 4 and 5, the formation of primer dimers can be seen.

Alternative methods to visualise diagnostic results exist however, these include lateral flow dipsticks (LFD) that make use of biotinylated primers and a streptavidin coated paper strip[100] this method seems simpler and should be explored in future studies. This method would make use of a simple two step experiment, the first being the RPA reaction step, where biotin molecules would be attached to the specific amplification primers. The second step would entail the introduction of a lateral flow dipstick that would interact with a biotinylated RPA amplicon, and indicate a positive result in the form of a visual line.

Chapter 5 – General Conclusion

The aim of this study was to establish new diagnostic methods, based on isothermal recombinase polymerase amplification (RPA) assays, for the detection of *Candidatus* Phytoplasma asteris (AY) and *Coniella granati*. Furthermore, this study aimed to compare polymerase chain reaction (PCR) diagnostic assays to. Moreover, this study set out to lay the groundwork for connecting the new diagnostic methods with a microfluidic device.

During this study a control construct was synthesised that consisted of a pGEM T-easy vector and partial 16S AY rDNA, known as the aster yellows control construct (AYCC). The AYCC was used to compare the diagnostic abilities of the RPA vs PCR. Diagnostic tests showed that the PCR diagnostics was approximately 10x more sensitive than the RPA. This may be due to the *Escherichia coli* cell components of plasmid extraction having RPA inhibitory characteristics, as suggested by the manufacturer[93]. However, the RPA diagnostic could detect the AYCC in ten minutes, and results were verifiable in 50 minutes, as opposed to the almost two hours of the PCR diagnostic. Cost implications regarding RPA vs PCR when compared 1:1, show an estimated cost of RPA:PCR being 119.80:12.24 ZAR with PCR diagnostics working out significantly cheaper than that of the RPA.

The main aim of this study was to develop new diagnostic techniques for the detection of AY phytoplasma and *C*. *granati* by means of RPA. This study demonstrates the successful development and implementation of both new diagnostic assays. The AY RPA diagnostic assay was successful in detecting AY phytoplasma. An advantage of using this RPA diagnostic assay as demonstrated in this study, is that the AY RPA can successfully detect AY phytoplasma in an hour and twenty minutes. The AY nested-PCR assay, however, takes up to ten hours for a definitive result.

This study also developed both a non-nested-PCR approach for the detection of *C*. *granati*, as well as an RPA diagnostic assay for the detection of the fungus. Once again, the RPA diagnostic was faster at detecting *C*. *granati* than the PCR, saving an estimated hour from start to finish.

This study also laid the groundwork for the RPA diagnostic assays to be attached to a microfluidic or electronic device. This was done by developing biotinylated oligonucleotide capture probes, complementary to the RPA amplicons. These probes were tested using streptavidin-magnetic beads/microspheres and could successfully

capture the desired product. Currently, probes are being attached to a streptavidin-coated electronic device and tested for their ability to capture the RPA amplicon and report a positive digital signal, at the department of Electronic and Electrical Engineering at Stellenbosch University.

This study investigated new diagnostic methods that could be implemented on-site in the future, without the requirement of a laboratory. However, not all avenues were explored, one of these avenues being the efficacy testing of probes that were already attached to a streptavidin surface. Another avenue that should be explored is the viability of RPA lateral flow dipsticks in detecting these specific plant pathogens. It is imperative that someone doing a similar study in the future look into this technique.

Finally, this research project contributes to the knowledge of new and developing diagnostic assays and their efficacy in detecting plant pathogens such as aster yellows phytoplasma and *Coniella granati*, as set out in the aims. Furthermore, from a biological perspective, sensitive and specific probes were designed and tested for use in an electronic device. This project was done in collaboration with the department of Electronic and Electrical Engineering at Stellenbosch University, to develop a system which combines both RPA diagnostic assays and electronic devices. As of the completion of this study successful results have been reported regarding the electronic device.

Future research projects should focus on the alternative methods as described in this thesis, such as testing infected plant material using the RPA diagnostic assays. As well as testing alternative RPA cleaning methods and alternative probe testing, to determine if more efficient methods exist.

Bibliography

1. SA wine industry 2017 statistics nr 42. (2018). Available at: http://www.sawis.co.za/info/download/Book_2016_statistics_year_english_final.pdf . (Accessed: 20th September 2018)
2. *Final Report - Macro-economic Impact of the Wine Industry on the South African Economy (also with reference to the Impacts on the Western Cape)*. 88 (2015).
3. Goosen, N. Pomegranate Industry Overview 2017. (2017). Available at: https://www.sapomegranate.co.za/wp-content/uploads/2017/11/POMASA-Presentation-27.10.2017.pptx.pdf. (Accessed: 29th May 2018)
4. Phaleng, C. L. & Lubinga, M. *South African Fruit Trade Flow 30 June 2018*. 13 (National Agricultural Marketing Council, 2018).
5. Carstens, R. *Aster Yellows disease in vineyards in South Africa*. (ARC Infruitec/Nietvoorbij, 2008).
6. van der Vyver, A. Investigating the recovery phenotype phenomenon in Aster Yellows phytoplasma-infected grapevine. (Stellenbosch University, 2017).
7. Cintora-Martínez, E. A. *et al.* Pomegranate fruit rot caused by Pilidiella granati in Mexico. *Australasian Plant Disease Notes* **12**, (2017).
8. Michailides, T. J., Puckett, R., Reyes, H. & Morgan, D. P. Fruit decay caused by Pilidiella granati in California. *Phytopathology* **100**, (2011).
9. Yang, X. *et al.* Development of a nested-PCR assay for the rapid detection of Pilidiella granati in pomegranate fruit. *Sci Rep* **7**, (2017).
10. Brzin, J. *et al.* Detection of apple proliferation phytoplasma by ELISA and PCR in growing and dormant apple trees. *J Plant Dis Prot* **110**, 476–483 (2003).
11. Londoño, M. A., Harmon, C. L. & Polston, J. E. Evaluation of recombinase polymerase amplification for detection of begomoviruses by plant diagnostic clinics. *Virol J* **13**, (2016).

12. Sakai, K. *et al.* Identification of Fungal Pathogens by Visible Microarray System in Combination with Isothermal Gene Amplification. *Mycopathologia* **178**, 11–26 (2014).
13. Kersting, S., Rausch, V., Bier, F. F. & von Nickisch-Rosenegk, M. Rapid detection of Plasmodium falciparum with isothermal recombinase polymerase amplification and lateral flow analysis. *Malaria Journal* **13**, 99 (2014).
14. Jauset-Rubio, M. *et al.* Ultrasensitive, rapid and inexpensive detection of DNA using paper based lateral flow assay. *Scientific Reports* **6**, 37732 (2016).
15. Lutz, S. *et al.* Microfluidic lab-on-a-foil for nucleic acid analysis based on isothermal recombinase polymerase amplification (RPA). *Lab Chip* **10**, 887–893 (2010).
16. WHO | Increasing fruit and vegetable consumption to reduce the risk of noncommunicable diseases. *WHO* Available at: http://www.who.int/elena/titles/fruit_vegetables_ncds/en/. (Accessed: 1st June 2018)
17. Slavin, J. L. & Lloyd, B. Health Benefits of Fruits and Vegetables1. *Adv Nutr* **3**, 506–516 (2012).
18. PEM, D. & JEEWON, R. Fruit and Vegetable Intake: Benefits and Progress of Nutrition Education Interventions- Narrative Review Article. *Iran J Public Health* **44**, 1309–1321 (2015).
19. Yadav, M. *et al.* Biological and Medicinal Properties of Grapes and Their Bioactive Constituents: An Update. *Journal of Medicinal Food* **12**, 473–484 (2009).
20. Mezni, A., Aoua, H., Khazri, O., Limam, F. & Aouani, E. Lithium induced oxidative damage and inflammation in the rat's heart: Protective effect of grape seed and skin extract. *Biomedicine & Pharmacotherapy* **95**, 1103–1111 (2017).

21. Nassiri-Asl, M. & Hosseinzadeh, H. Review of the Pharmacological Effects of Vitis vinifera (Grape) and its Bioactive Constituents: An Update. *Phytotherapy Research* **30**, 1392–1403 (2016).
22. Pomegranate. *University of Maryland Medical Center* Available at: http://umm.edu/health/medical/altmed/herb/pomegranate?utm_medium=social&utm_campaign=postplanner&utm_source=facebook.com. (Accessed: 13th March 2017)
23. Zarfeshany, A., Asgary, S. & Javanmard, S. H. Potent health effects of pomegranate. *Adv Biomed Res* **3**, (2014).
24. *Food Trade SA: The South African food trade and supply chain directory 2015*. 4 (Department of Agriculture, Forestry and Fisheries, 2016).
25. Doi, Y., Teranaka, M., Yora, K. & Asuyama, H. Mycoplasma- or PLT Group-like Microorganisms Found in the Phloem Elements of Plants Infected with Mulberry Dwarf, Potato Witches' Broom, Aster Yellows, or Paulownia Witches' Broom. *Japanese Journal of Phytopathology* **33**, 259–266 (1967).
26. Candidatus Phytoplasma asteris (yellow disease phytoplasmas). *Invasive Species Compendium* (2018). Available at: https://www.cabi.org/isc/datasheet/7642#tab1-nav. (Accessed: 5th June 2018)
27. Maramorosch, K. Historical reminiscences of phytoplasma discovery. *Bulletin of Insectology* **64**, 5–8 (2011).
28. Jackson, R. S. 4 - Vineyard Practice. in *Wine Science (Fourth Edition)* 143–306 (Academic Press, 2014). doi:10.1016/B978-0-12-381468-5.00004-X
29. Gibb, K. S., Constable, F. E., Moran, J. R. & Padovan, A. C. Phytoplasmas in Australian grapevines - detection, differentiation and associated diseases. *Vitis* **38**, 107–114 (1999).

30. Padovan, A. C. *et al.* Molecular detection of the Australian grapevine yellows phytoplasma and comparison with grapevine yellows phytoplasmas from Italy. *Australian Journal of Grape and Wine Research* **1**, 25–31
31. Fiore, N. *et al.* Molecular characterization of phytoplasmas in Chilean grapevines. *Bulletin of Insectology* **60**, 331–332 (2007).
32. Gajardo, A. *et al.* Phytoplasmas Associated with Grapevine Yellows Disease in Chile. *Plant Disease* **93**, 789–796 (2009).
33. Geographical distribution of Bois Noir phytoplasmas infecting grapevines in Croatia. (2000). Available at: https://www.cabi.org/isc/abstract/20001006481. (Accessed: 5th June 2018)
34. Daire, X., Clair, D., Larrue, J., Boudon-Padieu, E. & Caudwell, A. Diversity among mycoplasma-like organisms inducing grapevine yellows in France. *Vitis* **32**, 159–163 (1993).
35. Maixner, M., Ahrens, U. & Seemüller, E. Detection of Mycoplasmalike Organisms associated with a Yellows Disease of Grapevine in Germany. *Journal of Phytopathology* **142**, 1–10
36. Davis, R. E., Dally, E. L., Tanne, E. & Rumbos, I. C. Phytoplasmas Associated with Grapevine Yellows in Israel and Greece Belong to the Stolbur Phytoplasma Subgroup, 16SrXII-A. *Journal of Plant Pathology* **79**, 181–187 (1997).
37. Kolbe, M. *et al.* Occurrence of grapevine yellows disease in grapevine growing regions of Hungary. in *Proceedings 12th Meeting of the International Council for the Study of Viruses and Virus-Like Diseases of Grapevine (ICVG)* 73–74 (1997).
38. Mirchenari, S. M., Massah, A. & Zirak, L. 'Bois noir': new phytoplasma disease of grapevine in Iran. *Journal of Plant Protection Research* **55**, (2015).

39. Alma, A. *et al.* Mixed infection of grapevines in northern Italy by phytoplasmas including 16S rRNA RFLP subgroup 16SrI-B strains previously unreported in this host. *Plant Disease* **80**, 418–421 (1996).
40. Parente, A. M., Abreu, I. & Salema, R. Mycoplasma-like organisms associated with phloem cells of diseased grapevines in northern Portugal / Mykoplasma-ähnliche Organismen in Phloemzellen von erkrankten Weinreben im nördlichen Portugal. *Zeitschrift für Pflanzenkrankheiten und Pflanzenschutz / Journal of Plant Diseases and Protection* **101**, 124–127 (1994).
41. Saric, A., Skoric, D., Bertaccini, A., Vibio, M. & Murari, E. Molecular detection of phytoplasmas infecting grapevines in Slovenia and Croatia. in *Proceedings 12th Meeting of the International Council for the Study of Viruses and Virus-Like Diseases of Grapevine (ICVG)* 61–64 (1997).
42. Engelbrecht, M., Joubert, J. & Burger, J. T. First Report of Aster Yellows Phytoplasma in Grapevines in South Africa. *Plant Disease* **94**, 373–373 (2010).
43. Krüger, K. *et al.* Aster yellows phytoplasma in grapevines: identification of vectors in South Africa. 2
44. Plant Disease 1995 | First Report of Grapevine Bois Noir Phytoplasrna in Spain. Available at: https://www.apsnet.org/publications/PlantDisease/BackIssues/Documents/1995Abstracts/PD_79_1075C.htm. (Accessed: 6th June 2018)
45. Daire, X., Clair, D., Larrue, J. & Boudon-Padieu, E. Survey for grapevine yellows phytoplasmas in diverse European countries and Israel. *Vitis* **36**, 53–54 (1997).
46. Kessler, S. *et al.* Host plant preferences of Hyalesthes obsoletus, the vector of the grapevine yellows disease ‘bois noir’, in Switzerland. *Entomologia Experimentalis et Applicata* **139**, 60–67

47. Canik, D., Ertunc, F., Paltrinieri, S., Contaldo, N. & Bertaccini, A. Identification of different phytoplasmas infecting grapevine in Turkey. 2

48. Prezelj, N. *et al.* Metabolic Consequences of Infection of Grapevine (Vitis vinifera L.) cv. “Modra frankinja” with Flavescence Dorée Phytoplasma. *Front. Plant Sci.* **7**, (2016).

49. Lee, I.-M., Davis, R. E. & Gundersen-Rindal, D. E. Phytoplasma: Phytopathogenic Mollicutes. *Annual Review of Microbiology* **54**, 221–255 (2000).

50. Lee, I.-M., Bottner-Parker, K. D., Zhao, Y., Davis, R. E. & Harrison, N. A. Phylogenetic analysis and delineation of phytoplasmas based on secY gene sequences. *International Journal of Systematic and Evolutionary Microbiology* **60**, 2887–2897 (2010).

51. Jung, H.-Y., Chang, M.-U., Lee, J.-T. & Namba, S. Detection of “Candidatus Phytoplasma asteris” associated with henon bamboo witches’ broom in Korea. *Journal of General Plant Pathology* **72**, 261–263 (2006).

52. Sparks, M. E., Bottner-Parker, K. D., Gundersen-Rindal, D. E. & Lee, I.-M. Draft genome sequence of the New Jersey aster yellows strain of ‘Candidatus Phytoplasma asteris’. *PLOS ONE* **13**, e0192379 (2018).

53. Tran-Nguyen, L. T. T., Kube, M., Schneider, B., Reinhardt, R. & Gibb, K. S. Comparative Genome Analysis of “Candidatus Phytoplasma australiense” (Subgroup tuf-Australia I; rp-A) and “Ca. Phytoplasma asteris” Strains OY-M and AY-WB. *J. Bacteriol.* **190**, 3979–3991 (2008).

54. U. Seemüller, E. *et al.* Current status of molecular classification of the phytoplasmas. *Journal of Plant Pathology* **80**, (1998).

55. Seruga Musić, M. *et al.* Multilocus sequence analysis of ‘Candidatus Phytoplasma asteris’ strain and the genome analysis of Turnip mosaic virus co-infecting oilseed rape. *J. Appl. Microbiol.* **117**, 774–785 (2014).

56. Lee, I.-M. *et al.* 'Candidatus Phytoplasma asteris', a novel phytoplasma taxon associated with aster yellows and related diseases. *International Journal of Systematic and Evolutionary Microbiology* **54**, 1037–1048 (2004).

57. Zambon, Y., Contaldo, N., Richards, R. S., Bertaccini, A. & Burger, J. Multigene characterization of aster yellows phytoplasmas infecting grapevine in South Africa. *Phytopathogenic Mollicutes* **5**, S21 (2015).

58. Nisbet, C., Ross, S., Monger, W. A., Highet, F. & Jeffries, C. First report of '*Candidatus* Phytoplasma asteris' in commercial carrots in the United Kingdom. *New Dis. Reps.* **30**, 16–16 (2014).

59. Jarzembowski, P., Berniak, H., Faltyn, A., Jakubska-Busse, A. & Proćków, J. First Report of 'Candidatus Phytoplasma asteris' Associated with "Witches'-Brooms" on Jointleaf Rush (Juncus articulatus) in Poland. *Plant Disease* **99**, 281–281 (2014).

60. Klerk, R. de & Carstens, R. Aster yellows and leafhoppers. *Wineland Magazine* (2016).

61. Weintraub, P. G. & Beanland, L. Insect Vectors of Phytoplasmas. *Annual Review of Entomology* **51**, 91–111 (2006).

62. Leafhopper - an overview | ScienceDirect Topics. Available at: https://www.sciencedirect.com/topics/agricultural-and-biological-sciences/leafhopper. (Accessed: 7th June 2018)

63. Munyaneza, J. E. & Henne, D. C. Chapter 4 - Leafhopper and Psyllid Pests of Potato. in *Insect Pests of Potato* 65–102 (Academic Press, 2013). doi:10.1016/B978-0-12-386895-4.00004-1

64. Beanland, L., Hoy, C. W., Miller, S. A. & Nault, L. R. Influence of Aster Yellows Phytoplasma on the Fitness of Aster Leafhopper (Homoptera: Cicadellidae). *Ann Entomol Soc Am* **93**, 271–276 (2000).

65. Sanguez, J. Ontario CropIPM. *OMAFRA* (2009). Available at: http://www.omafra.gov.on.ca/IPM/english/grapes/diseases-and-disorders/phytoplasmas.html. (Accessed: 7th June 2018)

66. Moreira, L. *et al.* A phytoplasma associated with 'amachamiento' disease of dry common bean in Costa Rica. *Plant Pathology* **59**, 398–398

67. Dumonceaux, T. J., Green, M., Hammond, C., Perez, E. & Olivier, C. Molecular Diagnostic Tools for Detection and Differentiation of Phytoplasmas Based on Chaperonin-60 Reveal Differences in Host Plant Infection Patterns. *PLoS One* **9**, (2014).

68. Pérez-López, E., Rodríguez-Martínez, D., Olivier, C. Y., Luna-Rodríguez, M. & Dumonceaux, T. J. Molecular diagnostic assays based on cpn60 UT sequences reveal the geographic distribution of subgroup 16SrXIII-(A/I)I phytoplasma in Mexico. *Scientific Reports* **7**, 950 (2017).

69. Angelini, E., Luca Bianchi, G., Filippin, L., Morassutti, C. & Borgo, M. A new TaqMan method for the identification of phytoplasmas associated with grapevine yellows by real-time PCR assay. *J. Microbiol. Methods* **68**, 613–622 (2007).

70. Nejat, N. & Vadamalai, G. Diagnostic techniques for detection of phytoplasma diseases: past and present. *Journal of Plant Diseases and Protection* **1**, 16–25 (2013).

71. Smyth, N. The determination pf the spatial and temporal distribution of Aster yellows phytoplasma in grapevine. (Stellenbosch University, 2015).

72. Chen, Y. *et al.* First Report of a Fruit Rot and Twig Blight on Pomegranate (Punica granatum) Caused by Pilidiella granati in Anhui Province of China. *Plant Disease* **98**, 695–695 (2013).

73. Thomidis, T. & Exadaktylou, E. First Report of Pilidiella granati on Pomegranate with Symptoms of Crown Rot in the Prefecture of Xanthi, Greece. *Plant Disease* **95**, 79–79 (2010).

74. Mincuzzi, A., Garganese, F., Ippolito, A. & Sanzani, S. M. First Report of Pilidiella granati Causing Postharvest Fruit Rot on Pomegranate in Southern Italy. *Journal of Plant Pathology* **98**, 377 (2016).

75. Mirabolfathy, M., Groenewald, J. Z. & Crous, P. W. First Report of Pilidiella granati Causing Dieback and Fruit Rot of Pomegranate (Punica granatum) in Iran. *Plant Disease* **96**, 461–461 (2011).

76. Lennox, C. L., Mostert, L., Venter, E., Laubscher, W. & Meitz-Hopkins, J. C. First Report of Coniella granati Fruit Rot and Dieback on Pomegranate in the Western Cape of South Africa. *Plant Disease* **102**, 821 (2018).

77. Palou, L., Guardado, A. & Montesinos-Herrero, C. First report of *Penicillium* spp. and *Pilidiella granati* causing postharvest fruit rot of pomegranate in Spain. *New Dis. Reps.* **22**, 21–21 (2010).

78. KC, A. N. & Vallad, G. E. First Report of Pilidiella granati Causing Fruit Rot and Leaf Spots on Pomegranate in Florida. *Plant Disease* **100**, 1238–1238 (2016).

79. Alvarez, L. V., Groenewald, J. Z. & Crous, P. W. Revising the Schizoparmaceae: Coniella and its synonyms Pilidiella and Schizoparme. *Studies in Mycology* **85**, 1–34 (2016).

80. Chen, Y. *et al.* First Report of a Fruit Rot and Twig Blight on Pomegranate (Punica granatum) Caused by Pilidiella granati in Anhui Province of China. *Plant Disease* **98**, 695–695 (2013).

81. Mirabolfathy, M., Groenewald, J. Z. & Crous, P. W. First report of Pilidiella granati causing dieback and fruit rot of pomegranate (Punica granatum) in Iran. *Plant Disease* **96**, 461–461 (2012).

82. Yang, X. *et al.* Development of a nested-PCR assay for the rapid detection of Pilidiella granati in pomegranate fruit. *Sci Rep* **7**, (2017).

83. Faedda, R. *et al.* Heart rot and soft rot of pomegranate fruit in southern Italy. *Acta Horticulturae* 195–198 (2016). doi:10.17660/ActaHortic.2016.1144.28

84. Ezra, D., Kirshner, B., Hershcovich, M., Shtienberg, D. & Kosto, I. Heart Rot of Pomegranate: Disease Etiology and the Events Leading to Development of Symptoms. *Plant Disease* **99**, 496–501 (2015).

85. Smith, L. Pomegranate growers no closer to solving tree dieback. *ABC Rural* (2014). Available at: http://www.abc.net.au/news/2014-04-15/pomegranate-decline-continues-1504/5391070. (Accessed: 14th March 2017)

86. KC, A. N. & Vallad, G. E. Pomegranate disease survey update: Applying what is currently known to improve disease management in the upcoming season. *The Vegetarian Newsletter: A Horticultural Sciences Department Extension Publication on Vegetable and Fruit Crops* (2015).

87. The TwistDx story. Available at: https://www.twistdx.co.uk/en/rpa/our-story. (Accessed: 3rd June 2018)

88. RPA - The versatile replacement to PCR. Available at: https://www.twistdx.co.uk/en/rpa. (Accessed: 3rd June 2018)

89. Lobato, I. M. & O'Sullivan, C. K. Recombinase polymerase amplification: Basics, applications and recent advances. *TrAC Trends in Analytical Chemistry* **98**, 19–35 (2018).

90. Euler, M. *et al.* Development of a Panel of Recombinase Polymerase Amplification Assays for Detection of Biothreat Agents. *J. Clin. Microbiol.* **51**, 1110–1117 (2013).

91. Wahed, A. A. E. *et al.* A Portable Reverse Transcription Recombinase Polymerase Amplification Assay for Rapid Detection of Foot-and-Mouth Disease Virus. *PLOS ONE* **8**, e71642 (2013).

92. Piepenburg, O., Williams, C. H., Stemple, D. L. & Armes, N. A. DNA Detection Using Recombination Proteins. *PLoS Biol* **4**, (2006).

93. TwistAmp® DNA Amplification Kits Combined Instruction Manual. *TwistDx™* Available at: https://www.twistdx.co.uk/docs/default-source/twistamp-manuals/ta01cmanual-combined-manual_revo_v1-3a.pdf?sfvrsn=6. (Accessed: 3rd June 2018)

94. TwistDx. *What is Recombinase Polymerase Amplification? - TwistDx*.

95. Rohrman, B. A. & Richards-Kortum, R. R. A paper and plastic device for performing recombinase polymerase amplification of HIV DNA. *Lab Chip* **12**, 3082–3088 (2012).

96. Lau, H. Y. & Botella, J. R. Advanced DNA-Based Point-of-Care Diagnostic Methods for Plant Diseases Detection. *Front Plant Sci* **8**, (2017).

97. Silva, G. *et al.* Rapid detection of potyviruses from crude plant extracts. *Analytical Biochemistry* **546**, 17–22 (2018).

98. Rojas, J. A., Miles, T. D., Coffey, M. D., Martin, F. N. & Chilvers, M. I. Development and Application of qPCR and RPA Genus- and Species-Specific Detection of Phytophthora sojae and P. sansomeana Root Rot Pathogens of Soybean. *Plant Disease* **101**, 1171–1181 (2017).

99. Sun, K. *et al.* Recombinase polymerase amplification combined with a lateral flow dipstick for rapid and visual detection of Schistosoma japonicum. *Parasites & Vectors* **9**, 476 (2016).

100. Sajid, M., Kawde, A.-N. & Daud, M. Designs, formats and applications of lateral flow assay: A literature review. *Journal of Saudi Chemical Society* **19**, 689–705 (2015).

101. Jia, T.-W. *et al.* Assessment of the age-specific disability weight of chronic schistosomiasis japonica. *Bull World Health Organ, Bull. World Health Organ* **85**, 458–465 (2007).

102. Tu, P.-A. *et al.* Development of a recombinase polymerase amplification lateral flow dipstick (RPA-LFD) for the field diagnosis of caprine arthritis-encephalitis virus (CAEV) infection. *Journal of Virological Methods* **243**, 98–104 (2017).

103. Yeh, E.-C. *et al.* Self-powered integrated microfluidic point-of-care low-cost enabling (SIMPLE) chip. *Science Advances* **3**, e1501645 (2017).

104. Staroscik, A. dsDNA copy number calculator. *URI Genomics & Sequencing Center* (2004). Available at: https://cels.uri.edu/gsc/cndna.html. (Accessed: 6th September 2018)

105. Streptavidin-Coated Microspheres Binding Biotinylated DNA. *Polysciences, Inc* (2013). Available at: http://www.polysciences.com/skin/frontend/default/polysciences/pdf/TDS%20753.pdf. (Accessed: 1st September 2018)

Addendum A

SupaQuick DNA Extraction Protocol

• Grind 100 mg material in liquid nitrogen and transfer to a 2 ml Eppendorf, add 25 mg PVP-10 and shake to mix

• Let liquid nitrogen evaporate before adding 1 ml preheated CTAB extraction buffer mixed with 3% (30 µl) β-mercaptoethanol and incubate in a water bath for 15 minutes @ 60°C

• Centrifuge at 13200 rpm for 10 minutes (4°C)

• Retain aqueous phase (±800 µl) into a new 2 ml Eppendorf

• Add 5 µl RNase A (Stock 10 mg/µl)

• Invert and incubate in a water bath/oven for 15 minutes at 37°C

• Add equal volume cold C:I (24:1) and invert

• Centrifuge at 13200 rpm for 10 minutes (4°C)

• Retain aqueous phase and transfer to a new Eppendorf

• Add 0.8 volume cold Isopropanol and invert

• Centrifuge at 13200 rpm for 5 minutes (4°C), remove supernatant – use pipette

• Wash with 500 µl cold 70% ethanol – centrifuge at 13200 rpm for 5 minutes

• Remove the 70% ethanol with pipette and spin down for another 2 minutes and pipette the ethanol that is left – repeat step if necessary

• Allow the pellet to air dry for 10 minutes

• Resuspend in ± 25-40 µl H_2O (volume dependent on pellet size and concentration) – store in fridge until pellet is dissolved

Addendum B

Aster Yellows Control Construct Sequence

5’-

AAAAGACCTAGCAATAGGTATGCTTAGGGAGGAGCTTGCGTCACATTAGTTAGTTG
GTGGGGTAAAGGCCTACCAAGACTATGATGTGTAGCCGGGCTGAGAGGTTGAAC
GGCCACATTGGGACTGAGACACGGCCCAAACTCCTACGGGAGGCAGCAGTAGGG
AATTTTCGGCAATGGAGGAAACTCTGACCGAGCAACGCCGCGTGAACGATGAAGT
ATTTCGGTACGTAAAGTTCTTTTATTAGGGAAGAATAAATGATGGAAAGGATCCTTA
TTGTTAGTTACCAGCACGTAATGGTGGGGACTTTAGCAAGACTGCCAGTGATAAAT
TGGAGGAAGGTGGGGACGACGTCAAATCATCATGCCCCTTATGACCTGGGCTACA
AACGTGATACAATGGCTGTTACAAAGGGTAGCTGAAGCGCAAGTTTTTGGCGAATC
TCAAAAAAACAGTCTCAGTTCGGATTGA-3’

Addendum C

Aster Yellows Recombinase Polymerase Amplification Amplicon

5’-

AAAAACTGTTTAGCTAGAGTAAGATAGAGGCAAGTGGAATTCCATGTGTAGTGGTA
AAATGCGTAAATATATGGAGGAACACCAGTAGCGAAGGCGGCTTGCTGGGTCTTT
ACTGACGCTGAGGCACGAAAGCGTGGGGAGCAAACAGGATTAGATACCCTGGTA
GTCCACGCCGTAAACGATGAGTACTAAACGTTGGGTAAAACCAGTGTTGAAGTTAA
CACATTAAGTACTCCGCCTGAGTAGTACGTACGCAAGTATGAAACTTAAAGGAATT
GACGGGACTCCGCACAAGCGGTGGATCATGTTGTTTAATTCGAAGGTACCCGAAA
AACCTCATACAGCTTTGCAGAAGCATGTCAAGACCTGG-3’

Addendum D

***Coniella granati* 18S ribosomal RNA gene, partial sequence; internal transcribed spacer 1, 5.8S ribosomal RNA gene, and internal transcribed spacer 2, complete sequence; and 28S ribosomal RNA gene, partial sequence**

5’-
TTTAAGGACACAAACCCAGATACCCTTTGTGAACTTATTCTTATATCGTTGCCTCGG
CGCTGAGCTGGGGGCTTCTTTCCAAGAAGCTCTCCCATGGTCTCTCGGGACGATG
GAGCAAGCCCGCCGGCGGCCCTTCTAAACTCTTGTTTTTCTTACGTATCTCTTCTG
AGTTATTCAAAACAAAATGAATCAAAACTTTCAACAACGGATCTCTTGGTTCTGGCA
TCGATGAAGAACGCAGCGAAATGCGATAAGTAATGTGAATTGCAGAATTCAGTGAA
TCATCGAATCTTTGAACGCACATTGCGCCCGCTGGAATTCCAGCAGGCATGCCTG
TTCGAGCGTCATTTCACCCCTCAAGCCTTGCTTGGTGTTGGAGCACTACCGTTTGT
ACAAAGCGGTAGGCTCTGAAATTCAGTGGCGGGCTCGCTAAGACTCTGAGCGTAG
TAGTTTATCACCTCGCTTTGGAAGGATTAGCGGTGCTCTTGCCGTAAAACCCCACC
AATTTCTGAATTTTGACCTCGGATC-3’